TECHNICAL REPORT STANDARD PAGE

1. Title and Subtitle
   Implementation of Semi-circular Bend (SCB) Test for QC/QA of Asphalt Mixtures

2. Author(s)
   Louay Mohammad, Ph.D., P.E. (WY), F. ASCE, Jun Liu, Ph.D., Wei Cao, Ph.D., Peyman Barghabany, Ph.D.

3. Performing Organization Name and Address
   Louisiana Transportation Research Center
   Louisiana State University
   Baton Rouge, LA 70808

4. Sponsoring Agency Name and Address
   Louisiana Department of Transportation and Development
   P.O. Box 94245
   Baton Rouge, LA 70804-9245

5. Report No.
   FHWA/LA.24/685

6. Report Date
   June 2024

7. Performing Organization Code
   LTRC Project Number: 19-4B
   SIO Number: DOTLT1000321

8. Type of Report and Period Covered
   Final Report
   June 2024

9. No. of Pages
   88

10. Supplementary Notes

Conducted in Cooperation with the U.S. Department of Transportation, Federal Highway Administration

11. Distribution Statement

Unrestricted. This document is available through the National Technical Information Service, Springfield, VA 21161.

12. Key Words
    SCB; QC/QA; cracking resistance; rheology; chemistry; aging.

13. Abstract

The growing use of recycled asphalt materials in asphalt pavement poses durability concerns due to the replacement of virgin asphalt binder with recycled binder. The current volumetric-based Superpave mixture design is insufficient in addressing these concerns. To supplement conventional volumetric design, performance-based testing was introduced to assess the cracking performance of asphalt mixtures. The *Louisiana DOTD Specifications for Roads and Bridges* recommend using the critical strain energy release rate, *Jc*, obtained from the semi-circular bend (SCB) test, as a complement to evaluate the cracking resistance of asphalt mixtures. However, the requirement of long-term aging (LTA) for SCB samples at 85°C for 5 days is time-consuming for quality control/assurance (QC/QA) practices. Therefore, estimating SCB *Jc* for long-term aged asphalt mixtures based on unaged asphalt binder and mixture properties is beneficial. The objective of this study was to develop practical methods to predict SCB *Jc* of LTA asphalt mixtures for use in QC/QA programs. Fourteen field asphalt mixtures from throughout Louisiana were selected for this study. Loose asphalt mixtures

were compacted, laboratory aged at 85°C for 0-, 2-, 5-, 7-, and 10-days, and followed by SCB testing. Asphalt binders were extracted and recovered from the aged SCB samples for chemical and rheological characterization. Chemical characterizations included Saturate, Aromatic, Resin, and Asphaltene (SARA) analysis, Fourier transform infrared spectroscopy (FTIR), and gel permeation chromatography (GPC) tests. The rheological tests performed were Superpave performance grading, frequency sweep, linear amplitude sweep (LAS), and multiple stress creep recovery (MSCR) tests. GPC analysis revealed changes in asphalt binder components with increased aging, while rheological characterization indicated a decrease in cracking resistance. SCB test results demonstrated a reduction in fracture resistance with increased aging. Stepwise regression analysis identified significant parameters correlated with SCB *Jc*, such as asphalt binder film thickness (FT), percent passing from sieve #4 (P_4), aging level (day), asphalt binder polymer modification level (PM), and effective asphalt binder content (P_{be}). An ANN model utilizing gradient descent backpropagation was developed, validated, and able to accurately predict the LTA fracture parameter SCB *Jc* of asphalt mixtures. In summary. two approaches were developed for the prediction of LTA SCB *Jc*: (1) a scaling factor than can be implemented to forecast SCB *Jc* at 5 days aging from SCB *Jc* at 0 days aging, and (2) a user-friendly interface for the proposed ANN model. Both approaches are recommended for implementation in the Louisiana DOTD's asphalt mixture QC/QA programs.

Project Review Committee

Each research project will have an advisory committee appointed by the LTRC Director. The Project Review Committee is responsible for assisting the LTRC Administrator or Manager in the development of acceptable research problem statements, requests for proposals, review of research proposals, oversight of approved research projects, and implementation of findings.

LTRC appreciates the dedication of the following Project Review Committee Members in guiding this research study to fruition.

LTRC Administrator/Manager

Samuel B. Cooper, III, Ph.D., P.E.

Materials Research Administrator

Members

Brian Owens

Luanna Cambas

Danny Smith

Phillip Graves

Jason Davis

Directorate Implementation Sponsor

Chad Winchester, P.E., DOTD Chief Engineer

Implementation of Semi-circular Bend (SCB) Test for QC/QA of Asphalt Mixtures

By
Louay Mohammad, Ph.D., P.E. (WY), F. ASCE
Jun Liu, Ph.D.
Wei Cao, Ph.D.
Peyman Barghabany, Ph.D.

Department of Civil and Environmental Engineering
Louisiana State University
Louisiana Transportation Research Center
Baton Rouge, LA 70808

LTRC Project No. 19-4B
SIO No. DOTLT1000321

Conducted for
Louisiana Department of Transportation and Development
Louisiana Transportation Research Center

June 2024

Executive Summary

Conventional asphalt mixture design methodologies such as Superpave, Marshall, and Hveem are commonly used to determine the optimal asphalt binder content. These methods rely on physical and volumetric laboratory measurements to ensure that the proportion and quantity of asphalt binder meet stability and durability requirements. However, as the use of recycled materials increases, there is a need to develop additional laboratory tests to assess the quality of asphalt binder and complement the Superpave volumetric mixture design procedure. An important component in successful mixture design is the balance between volumetric composition and material compatibility. Balanced asphalt mixture design offers innovation in designing mixtures for the performance and evaluation of design quality, relative to the anticipated performance, using a rational approach. The 2016 *Louisiana Department of Transportation and Development (DOTD) Specifications for Roads and Bridges* introduced the concept of balanced mixture design by incorporating the Hamburg wheel tracking (HWT) and semi-circular bend (SCB) tests to evaluate high and intermediate temperature performance, respectively. However, the state's quality control/assurance (QC/QA) specifications and practices have not been updated accordingly; they only consider volumetric properties to ensure that mixtures are produced as intended and perform as expected in the field. This research aims to address this gap by proposing a methodology to implement performance tests for rutting and cracking during the QC/QA phases in Louisiana, specifically focusing on the practical implementation of the SCB test.

In the asphalt mixture design process, the 2016 *Louisiana DOTD Specifications for Roads and Bridges* specify a criterion for the critical strain energy release rate (*Jc*) obtained from the SCB test for different traffic levels. Typically, the SCB test is conducted on compacted samples that have been conditioned according to AASHTO R 30, which involves subjecting the samples to a temperature of 85°C for 5 days to simulate long-term aging (LTA) in the laboratory. However, QC/QA practices are time-sensitive, making it impractical to include LTA SCB samples in these tests. Therefore, this research developed two approaches for the prediction of LTA SCB *Jc*: (1) a scaling factor to forecast SCB *Jc* at 5 days aging from SCB *Jc* at 0 days aging, and (2) a model using artificial neural network (ANN) methodology to predict the LTA SCB *Jc* of asphalt mixtures, incorporating variables such as aging duration, mixture volumetric properties, and the chemical and rheological characteristics of asphalt binders as inputs. Both approaches eliminate the need for the long-term conditioning of plant-produced asphalt mixture samples, making it practical for the implementation of the SCB test in QC/QA testing.

The objectives of this study were: (1) to develop a specification for the implementation of the SCB test during the field QC/QA phases of asphalt mixture production and construction, and (2) to develop prediction approaches for forecasting the LTA SCB *Jc* of asphalt mixtures. To achieve these goals, 14 field projects with a reliable plant record of mixture consistency were identified and selected throughout Louisiana. The 14 asphalt mixtures were compacted and subjected to laboratory oven aging at 85°C for varying durations (0-, 2-, 5-, 7-, and 10-days), followed by SCB testing. Asphalt binders were extracted and recovered from the aged SCB samples for chemical and rheological characterization. Chemical characterization involved Saturate, Aromatic, Resin, and Asphaltene (SARA) analysis, Fourier transform spectroscopy (FTIR), and gel permeation chromatography (GPC) tests. Rheological tests included Superpave performance grading, frequency sweep, linear amplitude sweep (LAS), and multiple stress creep recovery (MSCR) tests. The GPC analysis revealed that the maltene and high-molecular weight components (with molecular weight greater than 19,000 Dalton (> 19K)) of the asphalt binders decreased with increasing aging levels, while the medium-molecular weight and asphaltene components (with molecular weight between 3,000 and 19,000 Dalton (3-19K)) increased due to oxidative aging. The asphaltene content (from SARA analysis) and carbonyl index (*CI*, from FTIR analysis) of asphalt binders increased with longer aging durations. The ΔTc parameter obtained from the BBR test indicated larger negative values with increased aging levels, indicating a decrease in stress relaxation capability. SCB *Jc* exhibited a strong correlation with ΔTc and a moderate correlation with A_{LAS} (a parameter from the LAS test). These observations suggest a relationship between the molecular structure of the asphalt binder due to aging, the rheological characteristics of the asphalt binder, and the fracture properties of the asphalt mixture. Using the SCB *Jc* data with various aging days, a scaling factor was developed to project SCB *Jc* at 5 days aging from SCB *Jc* at 0 days aging.

A comprehensive materials database was constructed using the testing data from this research, along with data from existing studies. Statistical analysis of the collected data using the stepwise regression method identified several significant parameters for determining the SCB *Jc* of asphalt mixtures, including aging level, effective binder content (P_{be}), aggregate percentage passing the #4 sieve (P_4), asphalt binder film thickness (FT), and asphalt binder modification level (PM). The ANN approach, employing the gradient descent backpropagation process, proved effective in predicting the LTA SCB *Jc* of asphalt mixtures. The predictive ANN model accurately forecasted the fracture performance (LTA SCB *Jc*) of asphalt mixtures, as evidenced by a R^2 value of 0.95 and a root-mean-square deviation (RMSE) value of 0.042. Additionally, a user-friendly interface was developed for implementation in Louisiana DOTD's asphalt mixture QC/QA programs.

Abstract

The growing use of recycled asphalt materials in asphalt pavement poses durability concerns due to the replacement of virgin asphalt binder with recycled binder. The current volumetric-based Superpave mixture design is insufficient in addressing these concerns. To supplement conventional volumetric design, performance-based testing was introduced to assess the cracking performance of asphalt mixtures. The *Louisiana DOTD Specifications for Roads and Bridges* recommend using the critical strain energy release rate, *Jc*, obtained from the semi-circular bend (SCB) test, as a complement to evaluate the cracking resistance of asphalt mixtures. However, the requirement of long-term aging (LTA) for SCB samples at 85°C for 5 days is time-consuming for quality control/assurance (QC/QA) practices. Therefore, estimating SCB *Jc* for long-term aged asphalt mixtures based on unaged asphalt binder and mixture properties is beneficial. The objective of this study was to develop practical methods to predict SCB *Jc* of LTA asphalt mixtures for use in QC/QA programs. Fourteen field asphalt mixtures from throughout Louisiana were selected for this study. Loose asphalt mixtures were compacted, laboratory aged at 85°C for 0-, 2-, 5-, 7-, and 10-days, and followed by SCB testing. Asphalt binders were extracted and recovered from the aged SCB samples for chemical and rheological characterization. Chemical characterization included Saturate, Aromatic, Resin, and Asphaltene (SARA) analysis, Fourier transform infrared spectroscopy (FTIR), and gel permeation chromatography (GPC) tests. The rheological tests performed were Superpave performance grading, frequency sweep, linear amplitude sweep (LAS), and multiple stress creep recovery (MSCR) tests. GPC analysis revealed changes in asphalt binder components with increased aging levels, while the rheological characterization indicated a decrease in cracking resistance. SCB test results demonstrated a reduction in fracture resistance with increased aging. Stepwise regression analysis identified significant parameters correlated with SCB *Jc*, such as asphalt binder film thickness (FT), percent passing from sieve #4 (P_4), aging level (day), asphalt binder polymer modification level (PM), and effective asphalt binder content (P_{be}). An ANN model utilizing gradient descent backpropagation was developed, validated, and able to accurately predict the LTA fracture parameter SCB *Jc* of asphalt mixtures. In summary. two approaches were developed for the prediction of LTA SCB *Jc*: (1) a scaling factor that can be implemented to forecast SCB *Jc* at 5 days aging from SCB *Jc* at 0 days aging, and (2) a user-friendly interface for the proposed ANN model. Both approaches are recommended for implementation in Louisiana DOTD's asphalt mixture QC/QA programs.

Acknowledgments

The authors would like to acknowledge the support provided by the Louisiana Transportation Research Center (LTRC) and Louisiana Department of Transportation and Development (DOTD). The assistance of Paragon Technical Services, Inc., in performing SARA analysis is appreciated.

Implementation Statement

It is anticipated that the results of this study will provide guidance to state agencies in QC/QA processes to shorten the time required for asphalt mixture aging prior to the SCB test. Two approaches were developed for the prediction of LTA SCB *Jc*: (1) a scaling factor to forecast SCB *Jc* at 5 days aging from SCB *Jc* at 0 days aging, and (2) a model using artificial neural network (ANN) methodology to predict the LTA SCB *Jc* of asphalt mixtures, incorporating variables such as aging duration, mixture volumetric properties, and the chemical and rheological characteristics of asphalt binders as inputs. Both approaches eliminate the need for the long-term conditioning of plant-produced asphalt mixture samples, making it practical for the implementation of the SCB test in QC/QA testing.

Table of Contents

List of Tables

List of Figures

Introduction

Asphalt pavement is designed to withstand traffic loads while minimizing deterioration. Cracking is a significant distress that occurs in asphalt pavement, particularly at intermediate and low temperatures. The increased usage of sustainable materials, such as reclaimed asphalt pavement (RAP), in asphalt pavement can lead to high stiffness in the asphalt mixture due to the introduction of aged asphalt binder. This introduces concerns regarding durability that cannot be adequately addressed by the current volumetric-based Superpave asphalt mixture design [1-3].

To overcome this limitation, performance-based testing is being introduced to complement the conventional volumetric asphalt mixture design and assess the cracking and rutting performance of asphalt mixtures. The *Louisiana Department of Transportation and Development (DOTD) Specifications for Roads and Bridges* specify the semi-circular bend (SCB) test as a complementary method to evaluate cracking resistance [4-6]. The SCB test is performed on long-term aged (LTA) samples that undergo a 5-day conditioning process at 85°C to simulate the long-term aging of asphalt mixtures in the laboratory.

Currently, the quality control/quality assurance (QC/QA) specifications in Louisiana focus primarily on controlling the volumetric and physical properties of asphalt mixtures, without incorporating fundamental properties obtained from mechanistic tests to assess cracking resistance [7]. By implementing the SCB test in QC/QA procedures, the quality of asphalt mixtures in terms of cracking resistance can be monitored during production and construction.

However, a challenge arises from the requirement of a 5-day laboratory aging process for the SCB test, as stipulated by AASHTO R30, *Standard Practice for Laboratory Conditioning of Asphalt Mixtures*, to simulate long-term aging in the field. Clearly, a 5-day aging duration is impractical for the implementation of the SCB test in QC/QA procedures. Although several research studies have attempted to develop expedited laboratory aging methods, there is currently no reliable and practical method with a consensus on its effectiveness [8-9]. Therefore, there is a need to explore alternative approaches that can estimate the cracking resistance of long-term aged asphalt mixtures without the lengthy aging process.

Literature Review

Asphalt mixtures undergo both short-term and long-term aging processes. Short-term aging occurs during production and construction stages due to the high temperatures involved, while long-term aging continues throughout the service life of the pavement under the combined effects of traffic and environmental loading. As a composite material, the aging state of an asphalt mixture depends on various volumetric properties, including air voids, asphalt content, asphalt film thickness, and aggregate gradation. Aging significantly influences the performance of the material by causing changes in the physical and chemical properties of the asphalt binder.

This section provides a concise review of existing studies that have investigated the effects of oxidative aging on the physical/mechanical and chemical properties of asphalt binders and asphalt mixtures, with a particular focus on crack resistance. The aim is to explore the different testing methods, theories, and analysis approaches employed in these studies. Additionally, this review aims to survey the available aging indices that have been developed to characterize and track the aging states of asphalt binders and their correlation with the crack resistance of asphalt mixtures.

Numerous research studies have investigated the impacts of aging on asphalt binders and mixtures. Commonly employed physical/mechanical testing methods include Superpave performance grading, dynamic shear rheometer (DSR), and bending beam rheometer (BBR). These tests help evaluate the fundamental properties of asphalt binders and their responses to various stress conditions, such as stiffness and ductility. Chemical testing methods, such as Fourier transform infrared spectroscopy (FTIR), gel permeation chromatography (GPC), and SARA analysis, provide insights into the chemical composition and molecular structure changes of asphalt binders during aging.

Theoretical frameworks have been proposed to understand the mechanisms behind aging and its influence on crack resistance. These include the time-temperature superposition principle, which allows for the prediction of long-term aging effects based on short-term laboratory aging data. Additionally, models based on rheological properties, such as the master curve approach, have been developed to predict the performance of asphalt binders and mixtures under various loading conditions.

To characterize and track the aging states of asphalt binders, various aging indices have been developed. These indices aim to capture the changes in physical and chemical properties caused by aging and correlate them with the crack resistance of asphalt mixtures. Examples of aging indices include the delta Tc (ΔT_c), Glover-Rove (G-R) parameter, and R-index. These indices provide valuable information for assessing the susceptibility of asphalt mixtures to cracking and can be used in mixture design and quality control processes.

Oxidative Aging of Asphalt Binders

The aging of asphalt binder occurs during the asphalt mixture production process and continues through the service life of the pavement. In general, aging increases the stiffness of asphalt binder and leads to reduced cracking resistance of the asphalt mixture. The aging of asphalt binder can be attributed to several mechanisms, including oxidation, polymerization, volatilization, condensation, and structural morphological changes. Among these mechanisms, oxidative aging has been shown to be the principal reaction responsible for the hardening of asphalt in the road [8]. Standard laboratory aging protocols developed under the Strategic Highway Research Program (SHRP) were also focused on the simulation of oxidative aging in the laboratory by aging the asphalt materials at elevated temperatures [9-12].

Petersen et al. investigated the relationship between viscosity and chemical properties during the oxidative aging process on a group of asphalt binders from the SHRP materials library [8]. Results indicated that the studied asphalt binders showed similar aging kinetics, with an initial rapid reaction "spurt" followed by a slower, constant rate reaction. The slow and constant rate reaction was found to be the dominant aging reaction in the field. The formation of ketones and sulfoxides was reported to be the major reason contributing to the viscosity increase. Additionally, Petersen et al. also observed that asphalt binder aging reaction "quenched" at a limiting viscosity after a certain field service duration. It was indicated that asphalt aging slowed down or ceased after a certain aging level [13].

To simulate field aging in a laboratory, Bell et al. indicated that the elevated temperature and pressure of oxygen were able to accelerate the oxidative aging process of asphalt binder during the Strategic Highway Research Program (SHRP) study [14]. They reported that the oxidative aging progression was affected by asphalt mixture characteristics, including aggregates absorption properties, asphalt mixture densities, and asphalt film thickness. Thus, it is necessary to consider these factors when developing a laboratory aging protocol for asphalt mixtures. The standard laboratory asphalt mixture aging procedure that developed under the SHRP project, AASHTO R30, requires conditioning compacted specimens in a forced oven at 85°C for 5 days to simulate the long-term field aging in the laboratory [10].

Kim et al. conducted the National Cooperative Highway Research Program (NCHRP) Project 9-54, Long-Term Aging of Asphalt Mixtures for Performance Testing and Prediction [15]. The objective of this study was to develop a practical and efficient laboratory long-term aging method for asphalt mixture performance testing. This study investigated the conditioning of loose asphalt mixtures and compacted samples using the conventional forced draft oven and pressure aging vessel (PAV). In this study, loose mixture aging in the oven at 95°C was proposed as the optimum long-term aging procedure for performance testing. This aging method exhibited the highest aging efficiency without changing the chemical properties of asphalt binders. Besides, the field aging levels obtained from field cores were matched with loose mixture aging levels at 95°C to determine the laboratory loose mixture aging duration. Additionally, a series of laboratory aging duration maps to match 4, 8, and 16 years of field aging at depths of 6 mm, 20 mm, and 50 mm below the pavement surface under different climate conditions in the United States were developed. However, for locations in southern Louisiana, they recommended aging the loose asphalt mixture for 27 days to simulate 16 years of field aging at the depth of 6 mm below the pavement surface, which is not practical for industry implementation.

Chemical Characterization of Aged Asphalt Binder

Several chemical analyses that can be used to investigate the components and molecular transformation of asphalt binders during the oxidation aging process have been identified in this literature review. Researchers use high-pressure gel permeation chromatography (HP-GPC) to study the size distribution of molecules in asphalt binder. GPC performs the separation of molecules in a sample based on the sizes, or more specifically, the hydrodynamic volumes of the molecules, a technique analogous to the aggregate sieving process in which the largest molecules elute first, followed successively by smaller molecules. Use of GPC helps researchers characterize the microscopic properties of asphalt binder and link it to the macroscopic behavior of asphalt binder and asphalt mixture. Aging can degrade large molecules of polymer modifier into smaller molecular sizes, whereas aging in base asphalt binder can significantly increase the amount of large molecular size species and decrease those of medium and small molecular sizes [16]. The transformation of asphalt components due to oxidative aging provides a basis for explaining the physical/mechanical property changes.

Petersen conducted a study to investigate the role of sulfoxide formation on physical properties during oxidative age hardening in asphalt binders [11]. It was shown that sulfoxide functional groups increased during oxidative aging, which resulted in the increased viscosity of asphalt binders. Newcomb et al. used the continuous performance grades (high and low temperatures) and the FTIR carbonyl area obtained from extracted asphalt binders to evaluate the aging equivalence between field aging due to production and construction and laboratory short-term aging protocols [17]. The results showed that most short-term aging of asphalt binders and asphalt mixtures occurs during plant production, while the aging induced by the construction process (i.e., transportation, laydown, and compaction) may be insignificant.

Rheological Characterization of Aged Asphalt Binder

In early studies, the ductility of asphalt binders was reported to be a good indicator of their cracking susceptibility [18, 19]. The ductility was measured at a reduced temperature (near 15°C) and elongation rate of 1 cm/min. It was generally believed that significant cracking would occur when the ductility of asphalt binders is 3 cm or lower.

Glover investigated the effect of asphalt binder aging on long-term pavement cracking performance by characterizing asphalt binder aging in terms of rheological properties [20]. A Maxwell model consisting of a spring (linear elastic element) and a dashpot (viscous element) was utilized to simulate the viscoelastic behavior of asphalt binder (see Figure 1).

Figure 1. The Maxwell Model: An Elastic and Viscous Element in Series [20]

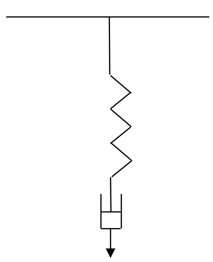

$$\tau + \frac{\eta_e}{E}\frac{d\tau}{dt} = \eta_e \frac{d\varepsilon}{dt}$$

where,

E = elastic modulus;

η_e= material coefficient of viscosity;

$\frac{d\tau}{dt}$ = rate of change in stress with respect to time;

$\frac{d\varepsilon}{dt}$ = rate of change in strain with respect to time.

The Maxwell model was applied to explain the viscoelasticity properties of asphalt binder. The elongation rate of 1 cm/min was found to be equivalent to the strain rate of approximately 0.005he s^{-1}. Moreover, it was found that the ratio of dynamic viscosity to the storage modulus (η'/G') and the value of the storage modulus G' were two parameters that represent the extension characteristics. The plotted map of G' versus η'/G' (measured at 15°C and 0.005 rad/s) was able to identify the different aging level. Additionally, it was found that the ductility obtained from the ductility test (15°C, 1 cm/min) correlated well with the dynamic shear rheometer (DSR) function of $G'/(\eta'/G')$ (determined at 15°C and 0.005 rad/s). Based on this finding, the DSR function of $G'/(\eta'/G')$ was proposed as a surrogate for the ductility of asphalt binders, as it is easier to obtain in the test compared with the ductility test. Further, the DSR function of $G'/(\eta'/G')$ was also recommended to represent the aging intensities induced in asphalt binders due to its sensitivity to asphalt aging levels.

Rowe demonstrated that $G'/(\eta'/G')$ was equivalent to $|G^*|\cos^2\delta/\sin\delta$, which has been referred to as the Glover-Rowe (G-R) parameter, as expressed in the following equation [21, 22].

$$\frac{G'}{\frac{\eta'}{G'}} = \frac{G'}{\frac{1}{\omega}\frac{G'}{G''}} = \frac{G'}{\frac{\tan\delta}{\omega}} = \frac{G^*(\cos\delta)^2}{\sin\delta}\,\omega \tag{1}$$

A master curve was used to obtain the required parameters to calculate G-R. The master curve characterizes the stiffness of asphalt binders over a wide range of frequency and temperatures. Figure 2 shows a typical master curve that utilizes the complex shear modulus, G*, and reduced frequency to describe the viscoelastic properties of asphalt binder as a function of time and temperature. Moreover, a mathematical model was used that can characterize the viscoelatic properties of asphalt binder, as shown in Equation (2) [23].

$$G^* = G_g\left[1 + \left(\frac{\omega_c}{\omega}\right)^{\frac{\log 2}{R}}\right]^{\frac{-R}{\log 2}} \tag{2}$$

Where,

$G^*(\omega)$ = complex shear modulus,

G_g = glass modulus (assumed equal to 1 GPa),

ω_r = reduced frequency at the defining temperature (rad/s),

ω_c = crossover frequency at the defining temperature (rad/s),

ω = frequency (rad/s), and

R = rheological index.

Figure 2. A Typical Master Curve and Physical Properties [24]

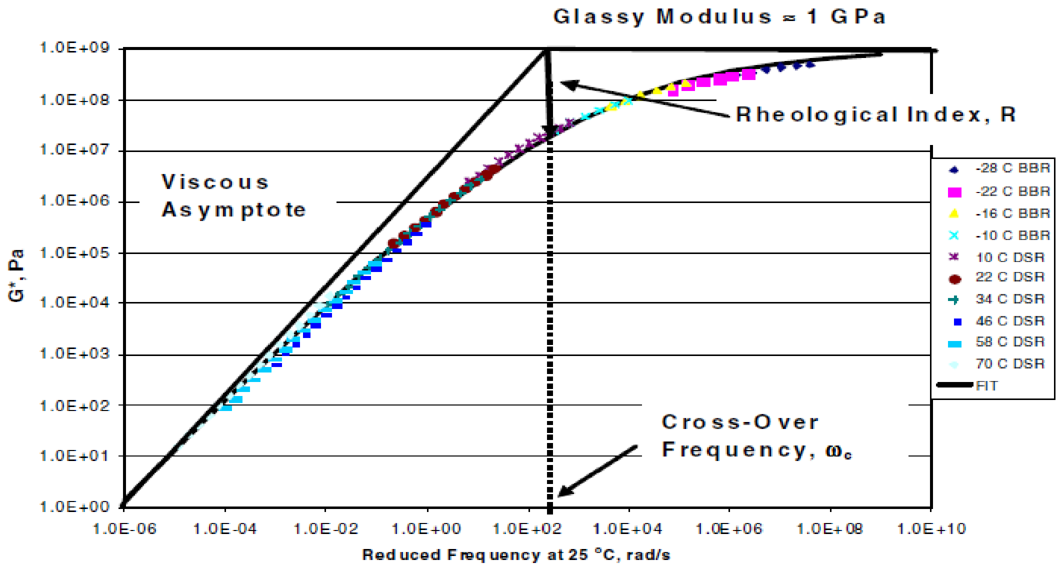

The master curve parameters (R and ω_c) have specific physical significance. The rheological index, R, is defined as the difference between the log of the glassy modulus and the log of the dynamic modulus at the crossover frequency. The R reduces with the stiffness. The crossover frequency, ω_c, is the frequency at which the storage modulus G' is equal to loss modulus G'', or where the phase angle is equal to 45°C. The modulus at crossover frequency is defined as crossover modulus. As the stiffness of asphalt binder increases, crossover frequency increases.

Semi-circular Bend (SCB) Test

Cracking is recognized as a major distress that decreases the service life of flexible pavements. Sufficient cracking resistance of asphalt mixtures is imperative to minimize the cracking potential of pavement. SCB test has been developed based on fracture mechanics to evaluate the cracking resistance of asphalt mixtures.

Test specimens with semi-circular geometry and a single-edge notch were first developed to measure the toughness of rock materials [25]. The *Jc*-integral concept, the nonlinear elastic energy release rate, was proposed by Rice [26], based on Paris law [27], to estimate strain concentration at smooth-ended notch tips in elastic and elastic-plastic materials. Equation (3) shows how the *Jc* -integral is calculated.

$$J_C = -\left(\frac{1}{b}\right)\frac{dU}{da} \tag{3}$$

Where,

Jc = critical strain energy release rate,

a = notch depth,

b = specimen thickness, and

U = total strain energy up to failure.

The SCB test and validity of *Jc* as a cracking resistance evaluation parameter has been widely studied and verified in numerical simulation, laboratory experiments, and field performance [15, 28-37].

Objective

The objective of this project was to establish a specification for the practical implementation of the semi-circular bend (SCB) test in the field QC/QA phases of asphalt mixture production and construction. The specific objectives of the study were to:

1. Investigate the impact of laboratory aging on the chemical and rheological properties of asphalt binders, as well as the cracking resistance of asphalt mixtures. This analysis will provide insights into the changes that occur in asphalt binders and mixtures as a result of aging.
2. Identify the statistically significant parameters that play a crucial role in predicting the critical strain energy release rate (SCB *Jc*) of asphalt mixtures due to aging. By determining these influential parameters, the study aims to enhance the accuracy of SCB *Jc* predictions.
3. Develop practical approaches for the prediction of LTA SCB *Jc* for QC/QA testing programs.

By accomplishing these objectives, this research will contribute to the establishment of a robust specification for incorporating the SCB test into the field QC/QA procedures of asphalt mixture production and construction. This specification will enhance the ability to assess and monitor the cracking resistance of asphalt mixtures, ensuring the long-term performance and durability of asphalt pavements.

Scope

In this study, 14 asphalt mixtures produced in asphalt plants and located on local and interstate roads in Louisiana were utilized. The characterization of each asphalt mixture was performed at the Louisiana Transportation Research Center (LTRC) asphalt laboratory.

Laboratory compaction was performed on the asphalt mixtures, and the compacted samples were subsequently subjected to aging at 85°C for five different durations: 0, 2, 5, 7, and 10 days. Following the aging process, the semi-circular bend (SCB) test, in accordance with ASTM D8044, was conducted on the samples to determine the output parameter, *Jc*. The SCB test provides crucial information about the cracking resistance of asphalt mixtures.

Upon completion of the SCB test, the asphalt binders were extracted and recovered from the aged samples. The auto extraction method, outlined in ASTM D8159, was employed for asphalt binder extraction, followed by the Abson method, in accordance with ASTM D1856, for the recovery process. Chemical and rheological characterizations of the recovered asphalt binders were then conducted.

To analyze the chemical properties of the recovered asphalt binders, Saturates Aromatics Resins Asphaltenes (SARA) analysis, Fourier transform infrared spectroscopy (FTIR) analysis, and gel permeation chromatography (GPC) tests were performed. These tests provide insights into the composition and chemical characteristics of the asphalt binders. The rheological properties of the recovered asphalt binders were also evaluated through various tests, including high temperature performance grade (HPG), bending beam rheometer (BBR), frequency sweep (FS), multiple stress creep recovery (MSCR), and linear amplitude sweep (LAS) tests. These tests enable the assessment of the rheological behavior and performance of the binders under different stress conditions.

Results obtained from asphalt binders' chemical and rheological characterizations, as well as SCB testing, were analyzed to develop practical approaches for the prediction of LTA SCB *Jc* for QC/QA testing programs.

Methodology

This chapter provides detailed descriptions of the asphalt materials utilized in this study, along with an overview of the testing methods employed for both asphalt binders and asphalt mixtures. Each test is accompanied by a concise review of its background, practical application, and data analysis procedures.

Materials

14 asphalt mixtures produced at various construction sites in Louisiana were included in this study (see Table 1). These mixtures were collected to represent the typical asphalt materials used in the region. The aggregates employed in the mixtures consisted of limestone and granite, which are commonly utilized in Louisiana and conform to the state's specification criteria for gradation.

The experimental factorial design encompassed the following factors:

- Asphalt Binder Types: Five types of asphalt binders were considered: PG 67-22 (unmodified), PG 70-22 (styrene-butadiene-styrene (SBS) modified), PG 70-22 (Latex modified), PG 76-22 (SBS modified), and PG 82-22 (Crumb Rubber modified). They represent different asphalt binder compositions commonly used in asphalt pavement construction.
- Asphalt Mixture Types: Two mixture types were investigated: dense-graded (HMA) and gap-graded (SMA).
- RAP materials: The studied asphalt mixtures contained RAP materials with content ranging from 0% to 26%.

The job mix formulas (JMFs) for the studied mixtures can be found in the Appendix. Typically, asphalt mixtures with finer gradation are utilized for the wearing course (WC) layer, which is the topmost layer of the pavement, responsible for withstanding traffic and providing a smooth riding surface. On the other hand, coarser asphalt mixtures are typically used for the binder course (BC) layer, which lies beneath the wearing layer and provides additional structural support to the pavement. By considering these various asphalt binder types, mixture types, and the inclusion of virgin and RAP materials, this research aims to investigate the impact of these factors on the performance of the asphalt mixtures. Based on the results of this investigation, the research team aims to build a comprehensive database containing data for asphalt mixtures using aggregates, asphalt binders, and modifiers commonly used by Louisiana DOTD.

Table 1. Asphalt Mixtures Composition

Mixture Designation	RAP Content (%)	Total %AC	Asphalt Binder PG	Modifier	V_a (%)	VMA (%)	VFA (%)	P_{be} (%)	D/B
M1-15RAP	15	5.0	70-22	SBS	3.5	14.7	76	4.8	0.96
M2-SMA	0	6.0	82-22	Crumb Rubber	3.5	16.3	79	5.5	1.31
M3-26RAP	26	4.6	76-22	SBS	3.5	13.2	73	4.1	1.02
M4-SMA	0	6.3	76-22	SBS	3.5	17	79	5.9	1.29
M5-18RAP	18	5.0	67-22	-	3.7	13.8	74	4.7	1.17
M6-18RAP	18	5.0	76-22	SBS	3.5	14.7	76	4.8	0.96
M7-15RAP	15	4.7	67-22	-	3.4	13.9	76	4.5	1.21
M8-15RAP	15	4.7	70-22	SBS	3.4	13.9	76	4.5	1.21
M9-28RAP	28	4.6	67-22	-	3.6	13.1	72	4.1	1.20
M10-20RAP	20	5.0	67-22	-	3.6	13.9	74	4.5	1.22
M11-19RAP	19	4.7	70-22	Latex	3.5	14.1	75	4.6	1.17
M12-19RAP	19	5.1	70-22	SBS	3.5	13.8	75	4.4	1.18
M13-SMA	0	6.3	76-22	SBS	3.7	16.5	78	5.6	1.47
M14-20RAP	20	4.2	70-22	SBS	3.5	12.5	72	3.8	0.92

Note: AC = asphalt content; PG = performance grade; V_a = air Voids; RAP = reclaimed asphalt pavement; VMA = voids in mineral aggregate; VFA = voids filled with asphalt; SBS = styrene butadiene styrene; P_{be} = effective asphalt binder; FT = film thickness; "-" means not available.

Asphalt Binder Experiment

Asphalt binders were extracted and recovered from the aged SCB specimens. These recovered binders were subjected to comprehensive characterization to assess their chemical and rheological properties. The characterization process involved various tests and analyses. For the chemical characterization, the Saturate, Aromatic, Resin, and Asphaltene (SARA) analysis was conducted. This analysis provides valuable information about the composition and distribution of different fractions within the asphalt binder. Additionally, the Gel Permeation Chromatography (GPC) test was performed to evaluate the molecular weight distribution of the binder components. Further, the Fourier-transform infrared spectroscopy (FTIR) test was employed to identify specific functional groups present in the binder and gain insights into its chemical structure.

For the rheological characterization, the Superpave performance-grading test was conducted. Additionally, the frequency sweep test was employed to assess the binder's viscoelastic properties across a range of frequencies. The linear amplitude sweep (LAS) test was performed to evaluate the binder's response to different strain amplitudes, aiding in understanding its ability to withstand intermediate-temperature cracking resistance. The multiple stress creep recovery (MSCR) test was conducted to assess the high-temperature properties of asphalt binders.

SARA Analysis

The SARA analysis determines the chemical composition of asphalt binder by fractionating it into saturates, aromatics, resins, and asphaltenes. Asphaltenes are defined operationally as the pentane- or heptane-insoluble component of asphalt binder, while maltenes are the soluble component that can be further separated into the other three fractions. Asphaltenes consist of extremely complex, highly polar molecules; they exhibit a very high tendency to associate into molecular clusters, and they play a significant role as viscosity builders in the rheology of asphalt binder [38]. During the oxidative aging process, ketones are formed, which significantly changes the polarity and solubility of the associated aromatic components, leading to their agglomeration to form the asphaltene component [39]. The resulting increase in the asphaltene fraction then becomes the primary reason for the increase in the asphalt viscosity due to aging [40]. Thus, in this study, the asphaltene fraction determined from the SARA analysis was used to evaluate the asphalt binder composition and cracking performance.

Based on the SARA results, an additional parameter referred to as the colloidal index can be obtained as the ratio of the sum of saturate and asphaltene contents to that of the resin and aromatic contents. This parameter was developed considering asphalt binder as a colloidal structure [41, 42]. A low colloidal index value indicates a well-dispersed system (i.e., the resins keep the highly associated asphaltenes dispersed in the light oily phase), which is more sol-like and homogeneous. A high colloidal index suggests a more gel-like system that is less dispersed and more heterogeneous. Asphalt binders with low colloidal indices are thus expected to exhibit better resistance to cracking due to their homogeneity and the free movement of the asphalt micelles [43]. The colloidal index was therefore utilized as another evaluation parameter in the SARA analysis.

Each recovered asphalt binder was first de-asphaltened in accordance with ASTM D3279 [44] to yield asphaltenes (insoluble) and maltenes (soluble). The maltene component was further fractionated on an Iatroscan TH-10 Hydrocarbon Analyzer to obtain the components of saturates, aromatics, and resins. The n-pentane was used to elute the saturates, and a 90/10 toluene/chloroform mixture was used to elute the aromatics. The resins were not eluted and remained at the origin.

FTIR Test

The FTIR test was conducted according to ASTM E1252 [45] for the identification and quantification of the functional groups present in asphalt binders. This approach was developed because molecules absorb light at the so-called resonant frequencies, which are characteristics of the covalent bonds in the molecules. By analyzing the position, shape, and intensity of peaks in the obtained infrared spectrum, details on the molecular structure of the asphalt can be revealed [46]. In this study, the carbonyl (C=O, a carbon atom double-bonded to an oxygen atom) was evaluated in relation to aging and cracking resistance. The underlying rationale is that highly polar and strongly interacting oxygen-containing functional groups, including carbonyl, are formed during the oxidative aging process. When the concentration of such polar functional groups becomes sufficiently high to cause molecular immobilization through increased intermolecular interaction forces, cracking will occur [47-49]. The carbonyl index (*CI*) is defined as the ratio indicated in Equation 4. Figure 3 shows a sample of FTIR test result for the recovered asphalt binder from mix 1 at 0-day aging level.

$$CI = \frac{Area\ of\ carbonyl\ band\ centered\ around\ 1700\ cm^{-1}}{\sum Areas\ of\ spectral\ bands\ between\ 1320\ and\ 1490\ cm^{-1}} \quad (4)$$

Figure 3. Sample FTIR spectrum

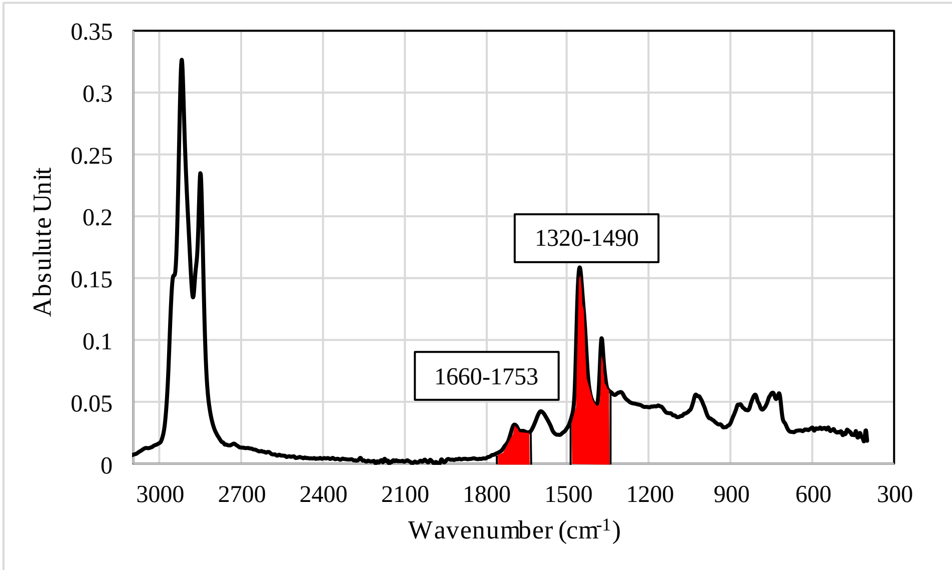

Gel Permeation Chromatography (GPC) Test

GPC analysis was performed according to ASTM D6579 [50] to determine the molecular weight distribution of the asphalt binders. Figure 4(a) presents a chromatogram of GPC test for the recovered asphalt binder from mix 1 at 0-day aging level. A calibration curve was used to convert elution time to molecular weight (MW) as shown in Figure 4(b). The chromatogram was then divided into four slices based on the molecular weight of the eluting species, Figure 4(c). Asphalt molecules are usually fractionated into three portions: high molecular weight (HMW) component (consisting of polymers and associated asphaltenes) with molecular weight greater than 19,000 Dalton (> 19K), asphaltene component with molecular weight between 3,000 and 19,000 Dalton (3-19K), and maltene component with molecular weight lower than 3,000 Dalton (< 3K). The percentage of asphaltene component (*%As*) was used as the evaluation parameter in the analysis.

Figure 4. (a) Gel Permeation Chromatography (GPC) Raw Curve, (b) Calibration Curve, and (c) Weight Distribution of Asphalt Binder Species.

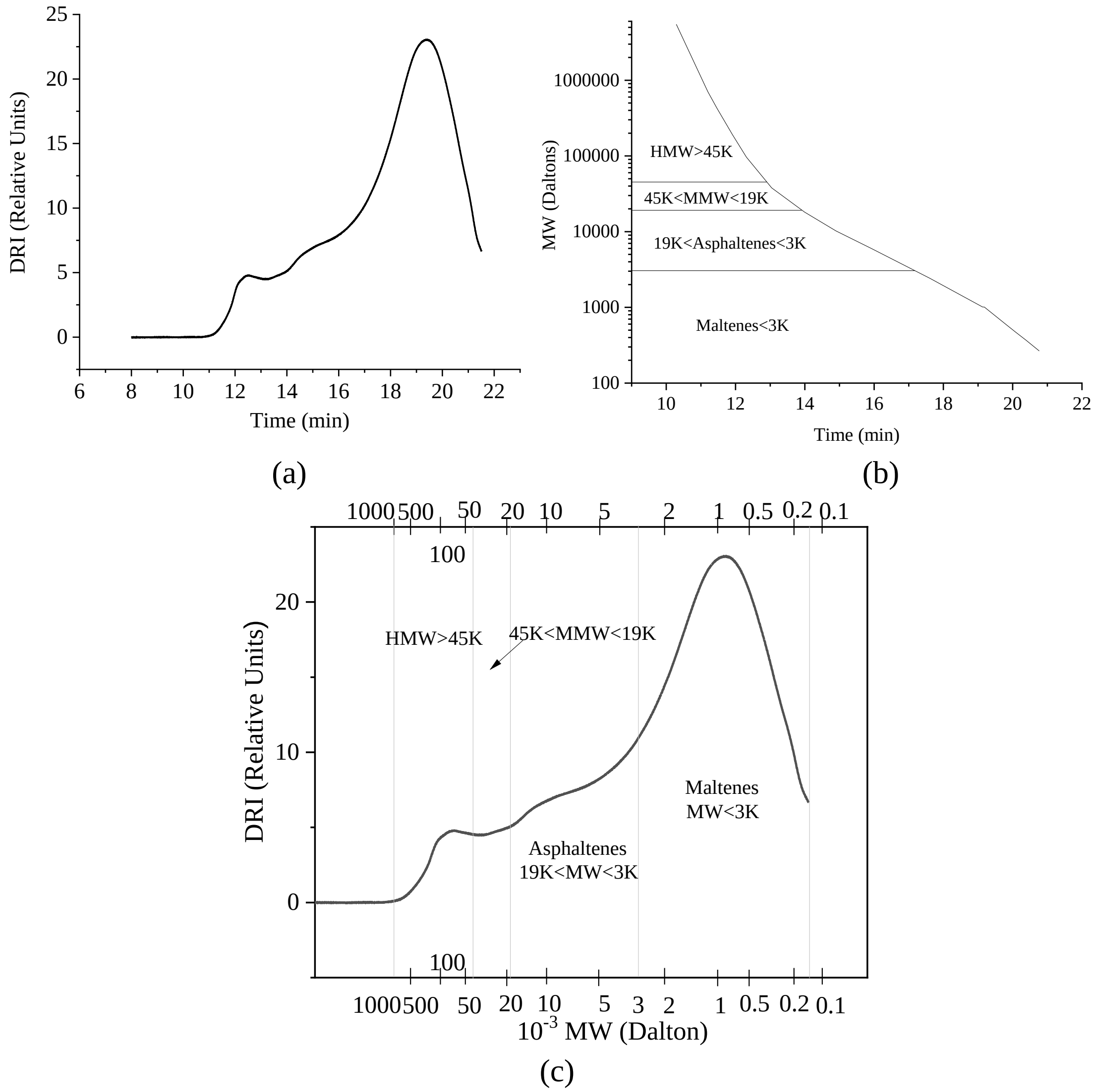

Note: DRI = change in refractive index; MW = molecular weight; MMW = medium molecular weight; HMW = high molecular weight.

Superpave Performance Grading

The Superpave performance grading consisted of high-temperature grading using a dynamic shear rheometer (DSR) following AASHTO R 29 [51] and low-temperature grading using a bending beam rheometer (BBR) following AASHTO T 313 [52]. In general situations for liquid asphalts, prior to grading, they should be first treated following the standard aging procedures through the rolling thin-film oven (RTFO) test according to AASHTO T 240 [53] and pressurized aging vessel (PAV) according to AASHTO R 28 [54]. In the present study, the asphalts to be graded were recovered from compacted mixture samples that had already been aged at different levels (i.e., 0-, 2-, 5-, 7-, and 10-days). For this reason, they were treated as RTFO-aged samples for the high-temperature grading and as PAV aged for the low-temperature grading; that is, no further aging treatment was applied to the recovered binders prior to performance grading. The performance grading results were then determined in accordance with AASHTO M 320 [53].

A rheological parameter that can be determined from the Superpave performance-grading test is the critical temperature difference denoted as ΔT_c, which is defined as:

$$\Delta T_c = T_S - T_m \tag{5}$$

Where, T_S is the critical temperature at which the flexural stiffness (S) of the beam equals 300 MPa, and T_m is the critical temperature at which the slope (m) of stiffness versus time in the log-log scale equals 0.300.

Note that both T_S and T_m were evaluated at a creep loading time of 60 seconds. Using the BBR test data, T_S and T_m can be obtained from interpolation following the practice specified in ASTM D7643 [54].

ΔT_c is an asphalt binder parameter that offers insights into the relaxation properties of the asphalt binder, which can contribute to non-load related cracking and other age-related embrittlement distresses. It has also been utilized as an indicator of how effectively asphalt binders respond to aging or how additives affect the asphalt binders' response to aging [55-60].

Frequency Sweep (FS) Test

The frequency sweep test was performed according to ASTM D7175 [61] to characterize the viscoelastic properties of asphalt binders at multiple temperatures, 15, 30, and 45°C, and various frequencies ranging from 0.1 to 100 rad/s. The Christensen Anderson (CA) model was used to fit a sigmoidal function on the test results [23, 62]. The effects of aging intensities on ductility properties were quantified with use of the Glower Rowe (G-R) parameter. The values of |G*| and δ at 15°C and 0.005 rad/s were first obtained from the fitted curves. Then, the G-R parameter was determined and used in the analysis using Equation 6 [22, 63].

$$\text{G-R Parameter} = \frac{|G^*| \times cos^2\delta}{sin\delta} \tag{6}$$

Where, G* is the shear complex modulus defined as the ratio of the shear stress to the shear strain at each cycle, and δ is the phase angle defined as the time lag between the applied shear strain and the measured shear stress in degree.

Linear Amplitude Sweep (LAS) Test

The LAS test was conducted at an intermediate temperature of 18°C in accordance with AASHTO TP 101 [64] to ascertain the fatigue resistance of asphalt binders. A parallel-plate geometry with an 8-mm diameter and a 2-mm gap was used. This test procedure consisted of frequency sweep followed by the amplitude sweep with a 1-min. interval for stress relaxation. The frequency sweep was performed at 0.1% strain over a frequency range of 0.1 to 30 Hz to obtain material properties at the intact state of the LAS test condition. The amplitude sweep had a constant frequency of 10 Hz and began with 100 cycles of sinusoidal oscillation at 0.1% strain. Each successive loading step comprised 100 cycles at strain amplitude linearly increasing from 1% to 30% at a rate of 1% per step.

The LAS data analysis was based on the viscoelastic continuum damage theory [65-67]. The analysis approach described in AASHTO TP 101 was critically reviewed and the formulation revised. A parameter denoted as A_{LAS} was developed and proposed as the indicator of asphalt binder fatigue resistance [68]. The following describes the development of the formulation and the A_{LAS} parameter.

Analogous to the S-VECD model applied to asphalt mixture fatigue characterization, the structural integrity of asphalt binder is represented by the normalized dynamic shear modulus:

$$C = \frac{|G^*|}{DMR \cdot |G^*|_{LVE}} \tag{7}$$

Where,
$|G^*|$ is the apparent dynamic shear modulus in the amplitude sweep test. It is calculated as the ratio of stress amplitude to strain amplitude for each cycle;
$|G^*|_{LVE}$ is the linear viscoelastic dynamic modulus corresponding to the LAS test temperature and frequency. It can be interpolated from the dynamic shear modulus master curve, Equation (8); and
DMR for asphalt binder is calculated as:

$$DMR = \frac{|G^*|_{0.1\%}}{|G^*|_{LVE}} \tag{8}$$

Where, $|G^*|_{0.1\%}$ is the dynamic modulus value obtained from the frequency sweep of the LAS test with 0.1% strain, which serves as the fingerprint of the sample.

The pseudo strain energy for asphalt binder is given by:

$$W^R = \frac{1}{2} DMR \cdot C(S) \cdot \left(\gamma^R(\xi)\right)^2 \tag{9}$$

Where, $\gamma^R(\xi)$ is the pseudo-shear strain time history given by:

$$\gamma^R(\xi) = \gamma \cdot |G^*|_{LVE} \cdot \sin\left(\omega_r \xi\right) \tag{10}$$

Where, γ denotes shear strain amplitude.

Combining Equations (9) and (10), making appropriate substitutions, and integrating over a cycle, the damage increment per cycle is calculated as:

$$\Delta S_i = \left[\frac{1}{2} DMR \cdot \left(\gamma_i \cdot |G^*|_{LVE}\right)^2 \left(C_{i-1} - C_i\right)\right]^{\frac{\alpha}{1+\alpha}} \cdot Q^{\frac{1}{1+\alpha}} \quad \text{with} \quad Q = \int_0^{2\pi/\omega_r} \left(\sin(\omega_r \xi)\right)^{2\alpha} d\xi \tag{11}$$

Where, α is determined according to AASHTO TP 101 as the exponent of the power-law fit to $|G^*|$ versus ω_r obtained from the frequency sweep step in the LAS test.

$$C(S) = 1 - C_1 S^{C_2} \tag{12}$$

$$\frac{dS}{d\xi} = \left(-\frac{\partial W^R}{\partial S} \right)^{\alpha} \tag{13}$$

The obtained C-S data pairs are then cross-plotted and fitted using the power-law form as shown in Equation (12). Substituting Equation (12) into Equation (13) and following a derivation procedure, one can obtain the following that can be used for fatigue simulation:

$$N_f = \left[\frac{1}{2} C_1 C_2 \cdot \left(|G^*|_{LVE} \right)^2 \right]^{-\alpha} \cdot (\kappa Q)^{-1} \cdot \left(S_f \right)^{\kappa} \cdot \gamma_0^{-2\alpha} \tag{14}$$

Where, $\kappa = 1 + \alpha - \alpha C_2$, and γ_0 is the strain amplitude for simulation. Note that the effect of loading condition (temperature and frequency) is incorporated in Q, as seen in its definition in Equation (11).

Equation (14) presents a power-law relationship between fatigue life N_f and strain input γ_0, which are related through a coefficient herein denoted as A_{LAS}:

$$A_{LAS} = \left[\frac{1}{2} C_1 C_2 \cdot \left(|G^*|_{LVE} \right)^2 \right]^{-\alpha} \cdot (\kappa Q)^{-1} \cdot \left(S_f \right)^{\kappa} \tag{15}$$

The A_{LAS} parameter is then proposed as an indicator of asphalt binder fatigue resistance. A higher A_{LAS} value is desired for the fatigue resistance of asphalt binders, as seen in Equation (15).

Multiple Stress Creep Recovery (MSCR) Test

MSCR test was conducted according to AASHTO T350 to characterize the creep and recovery characteristics of recovered asphalt binders at 64°C. The test was performed using a constant stress creep of 1.0s duration followed by a zero stress recovery of 9.0s duration. Two stress levels of 0.1 kPa and 3.2 kPa were applied for 20 and 10 cycles, respectively. Non-recoverable creep compliance ($J_{nr,\,3.2}$) and percent recovery ($\%R$), expressed in Equations (16) and (17), were used to characterize the rutting performance of the recovered STA asphalt binders.

$$J_{nr} = \frac{Non-recoverable\ strain}{Stress\ level} \tag{16}$$

$$\%R = \frac{Recoverable\ strain}{Total\ shear\ strain} \tag{17}$$

Asphalt Mixture Experiment

Semi-circular Bend (SCB) Test

The SCB test was conducted according to ASTM D8044 to evaluate the intermediate-temperature cracking resistance of asphalt mixtures. After compaction, samples were subjected to oven aging, 5 days at 85°C, prior to testing. The test was performed at a constant displacement rate of 0.5 mm/min at 25°C. The critical strain energy release rate, *Jc*, is used to ascertain the cracking resistance of asphalt mixtures. The critical strain energy release rate, *Jc*, is calculated using Equation (18):

$$Jc = -\left(\frac{1}{b}\right)\frac{dU}{da} \tag{18}$$

Where,
Jc is critical strain energy release rate (kJ/m^2),
b is sample thickness (m),
a is notch depth (m),
U is strain energy to failure (kJ), and
d*U*/d*a* is change of strain energy with notch depth (kJ/m).

Discussion of Results

This section is organized into five subsections, each addressing a specific aspect of the study. The subsections are asphalt binder test results, asphalt mixture test results, comparative analysis of the test results, database collection, and model development. In the first subsection, the test results for the asphalt binders are presented and analyzed. The second subsection focuses on the SCB test results obtained from the asphalt mixtures to assess the effects of aging levels on the mixtures' fracture behavior. The third subsection involves a comparative analysis of the test results, wherein the data from the asphalt binders and mixtures are examined together. This analysis enables a comprehensive understanding of the relationship between the binder properties and the corresponding performance of the asphalt mixtures. The fourth subsection presents and describes the database that was collected in this study. Given the diverse range of test methods employed in the study, significant parameters that have a strong correlation with the SCB *Jc* (critical strain energy release rate) were identified. In the fifth subsection, the development of practical approaches for the prediction of LTA SCB *Jc* for QC/QA testing programs is discussed. Two approaches are discussed specifically: (1) a scaling factor to forecast SCB *Jc* at 5 days 85°C aging from SCB *Jc* at 0 days aging (plant-produced mixtures), and (2) a model using artificial neural network (ANN) methodology to predict the LTA SCB *Jc* of asphalt mixtures, incorporating variables such as aging duration, mixture volumetric properties, and the chemical and rheological characteristics of asphalt binders as inputs.

Further, it is important to note that results obtained from the first eight mixtures (M1 to M8, Table 1) were specifically analyzed to investigate the impact of aging levels on the fracture cracking resistance of both the asphalt binders and mixtures. These results were then utilized to develop the ANN SCB *Jc* predictive model. To validate the accuracy and reliability of the developed ANN model, mixtures M9 to M14 (Table 1) were used for testing and verification purposes. This validation process allows for an assessment of the model's ability to accurately predict SCB *Jc* values for the long-term aged asphalt mixtures.

In order to statistically assess the difference between test results, a one-way ANOVA analysis using the F-test was performed. The null hypothesis for the F-test was that the average value of a specific test result would be the same for all mixtures. The alternative hypothesis was that the average of the test parameter for all mixtures would not be the same. If the null hypothesis was rejected, a post-hoc test was performed in order to make further comparison between test results. In this research, Fisher's least square difference (LSD) post-hoc test was performed to rank the laboratory test results. Letters A, B, C, D, and E were assigned to test results to show statistically distinct test results from best to worst.

Asphalt Binder Testing

This section presents the asphalt binder testing results, including chemical and rheological characterizations. Chemical evaluation was based on SARA fractionation, GPC, and FTIR tests. Rheological testing included the Superpave performance grading, frequency sweep, and linear amplitude sweep tests. All testing was performed on the asphalt binders extracted from the compacted asphalt mixture samples that were oven-aged at different aging levels.

SARA Analysis

The recovered asphalt binders were fractionated into saturates, aromatics, resins, and asphaltenes (SARA), and the results are given in Table 2. The asphaltene percentage varied in a narrow range for all recovered asphalt binder types except for M3-26RAP. The wider range of asphaltenes for M3-26RAP can be attributed to its higher RAP content and higher aging susceptibility. For all the recovered asphalt binders, 10-day aged samples yielded higher asphaltene concentration than 0-day aged samples. It is observed that higher asphaltene concentrations generally resulted in higher colloidal indices. In general, higher aging levels yielded asphalt binders with a less dispersed microstructure (higher colloidal index) that was expected to be more susceptible to cracking.

Table 2. SARA Analysis Results

Recovered asphalt binder type	Aging level (days)	Asphaltenes (%)	Resins (%)	Aromatics (%)	Saturates (%)	Colloidal Index
M1-15RAP	0	21.9	25.8	46.5	5.8	0.38
	2	21.8	26.2	45.3	6.7	0.40
	5	24.9	30.8	38.8	5.6	0.44
	7	23.8	26.7	43.9	5.6	0.42
	10	24.4	28.1	41.6	5.9	0.44
M2-SMA	0	23.4	23.4	47.6	5.6	0.41

Recovered asphalt binder type	Aging level (days)	Asphaltenes (%)	Resins (%)	Aromatics (%)	Saturates (%)	Colloidal Index
	2	23.5	23.4	48.0	5.0	0.40
	5	30.3	22.5	42.2	4.9	0.54
	7	25.5	25.3	43.5	5.7	0.45
	10	26.7	26.3	40.4	6.5	0.50
M3-26RAP	0	24.1	26.7	43.0	6.2	0.43
	2	24.3	24.4	44.6	6.7	0.45
	5	27.9	28.0	37.6	6.4	0.52
	7	28.3	27.0	37.6	7.0	0.55
	10	30.7	25.7	36.7	6.9	0.60
M4-SMA	0	23.7	22.8	46.0	7.5	0.47
	2	23.8	24.0	46.4	5.8	0.42
	5	23.0	23.2	47.4	6.4	0.42
	7	24.8	24.8	44.5	5.9	0.44
	10	25.5	23.5	45.3	5.7	0.45
M5-18RAP	0	19.5	25.8	47.8	6.9	0.36
	2	20.0	28.7	45.3	5.9	0.37
	5	20.3	27.6	45.7	6.4	0.36
	7	21.8	29.7	41.2	7.3	0.41
	10	22.4	29.3	40.6	7.7	0.43
M6-18RAP	0	25.3	29.0	39.2	6.5	0.47
	2	25.8	28.2	39.0	6.7	0.48
	5	26.9	27.2	38.9	7.0	0.51
	7	27.4	25.0	40.5	7.0	0.53
	10	28.9	28.0	35.6	7.5	0.57
M7-15RAP	0	22.8	26.8	43.9	6.5	0.41
	2	22.9	26.4	44.8	5.9	0.40
	5	24.7	27.8	40.7	6.7	0.46
	7	25.0	28.2	40.8	6.1	0.45
	10	25.0	28.6	39.6	6.7	0.46
M8-15RAP	0	20.1	28.9	44.6	6.4	0.36
	2	22.9	29.4	41.6	6.1	0.41
	5	24.8	29.6	39.3	6.3	0.45
	7	26.0	31.0	35.6	7.1	0.50
	10	26.3	31.5	38.6	6.9	0.47

FTIR Test

Figure 5 presents the carbonyl index (*CI*) results for asphalt binders at different aging levels. Higher *CI* values represent higher oxidation levels [46]. In general, higher *CI* values were observed as aging level increased. Statistical ranking within each mixture is shown in Figure 5. For each mixture, there was a significant increase in the *CI* value between 0-day and 2-day aging. The *CI* values for 5- and 7-day aging were comparable for most of the studied mixtures, such as mixes 1, 2, and 4. However, 10-day aging significantly increased the *CI* value. Mixture M2 showed the highest *CI* values at 10-day aging compared to other asphalt binders. This observation may be attributed to the usage of the crumb rubber modified asphalt binder (PG 82-22) in this mixture. Further, Mixture M7 showed the lowest *CI* values at 0-day aging level. This observation may be related to the application of softer asphalt binders compared to the other mixtures. In order to evaluate the aging susceptibility of asphalt mixtures, an aging index (AI) was used, which was defined as the ratio of the *CI* at a 10-day aging level to the *CI* at a 0-day aging level. A lower AI value means that the asphalt mixture exhibited a lower susceptibility to aging. It is noted that asphalt binders recovered from M2 showed relatively higher AI values compared to other asphalt binders. Further, asphalt binders recovered from mixture M4 showed the lowest AI values suggesting the effect of polymer modification on improving the aging susceptibility of the asphalt binder (PG 76-22). Previous studies also stated that polymer modification can improve the aging susceptibility of asphalt binders [69, 70]. Additionally, the recovered asphalt binder from M4, with a polymer-modified asphalt binder containing the highest effective asphalt binder content, yielded the lowest aging susceptibility.

Figure 5. FTIR Test Results

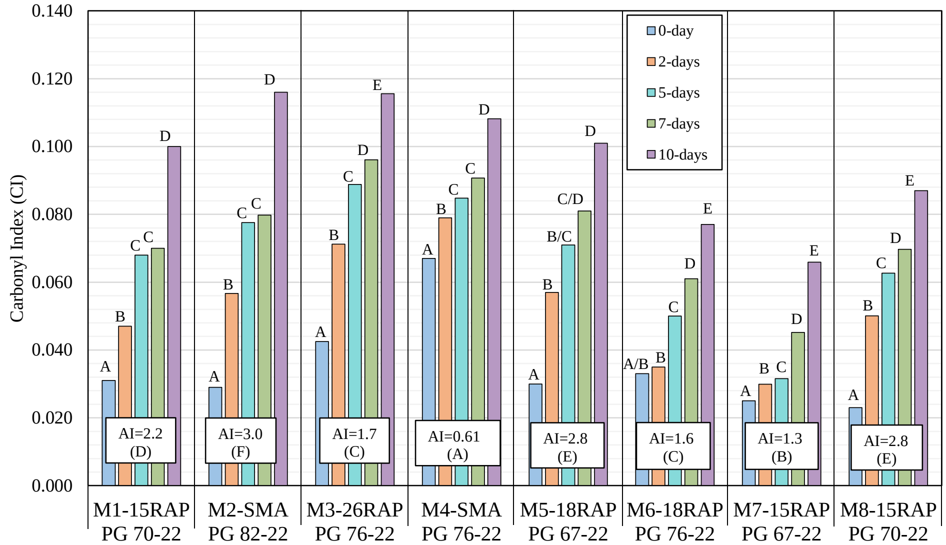

Gel Permeation Chromatography (GPC) Test

The GPC technique fractionates asphalt binder molecules based on the molecular sizes (based on elution time), which are then converted to molecular weight after calibration. Asphalt molecules are usually fractionated into three portions: high molecular weight (HMW) component (consisting of polymers and associated asphaltenes) with molecular weight greater than 19,000 Dalton (> 19K), asphaltene component with molecular weight between 3,000 and 19,000 Dalton (3-19K), and maltene component with molecular weight lower than 3,000 Dalton (< 3K). It should be acknowledged that the GPC and SARA techniques fractionate asphalt binders based on different properties (molecular size versus solubility) of the molecules, and thus the obtained results, such as asphaltene and maltene percentages, are not necessarily comparable. Table 3 presents the compositional analysis of the GPC test results for the asphalt binders at different aging levels. Note that statistical analysis was not performed on GPC test results because one replicate was available for each asphalt binder type. In general, for all asphalt binder types, maltene content decreased with aging, while asphaltene content increased because of incremental oxidative aging. Further, the percentage of medium molecular weight (with molecular weight between 3,000 and 19,000 Dalton) increased with aging, while high molecular weight content (with molecular weight greater than 19,000 Dalton) showed a decreasing trend with aging. This observation is attributed to the degradation of polymer species into smaller components due to oxidative aging [49]. Further, recovered asphalt binders from M3 and M4 showed relatively higher HMW components compared to other asphalt binders. Note that M4 showed the lowest AI values as measured by FTIR *CI* parameter, indicating asphalt binders with higher HMW contents had lower aging susceptibility. It was noted that asphalt binders recovered from mixes with unmodified asphalt binder (PG 67-22), such as M5 and M7, showed relatively lower HMW content. HMW components slightly decreased with an increase in aging level in M3 (PG 76-22) and M4 (PG 76-22). This observation is attributed to the degradation of polymer species into smaller components due to oxidative aging. However, there was no obvious trend in the change of HMW component for the other recovered asphalt binders when the aging level was increased. The GPC results revealed that there was no significant increase in the percentage of asphaltenes when the aging level increased from 2 to 5 days, for all the studied recovered asphalt binders. Additionally, the differences in HMW contents from 2 to 5 days aging for a given asphalt binder were insignificant. This implied that there was a balance between the association of low-molecular-weight components and dissociation of high-molecular-weight components when the aging level increased from 2 to 5 days.

Table 3. GPC Test Results

Recovered asphalt binder type	Aging level (days)	Maltenes% (<3K)	Asphaltenes% (3-19K)	MMW% (19-45K)	HMW% (>45K)
M1-15RAP	0	68.4	26.3	3.3	2.0
	2	67.8	26.8	3.5	1.9
	5	64.9	28.3	5.0	1.8
	7	64.3	28.9	5.1	1.7
	10	64.0	29.2	5.2	1.6
M2-SMA	0	65.7	29.9	3.2	1.3
	2	64.2	30.7	3.7	1.4
	5	62.5	31.6	4.3	1.6
	7	62.4	32.0	4.3	1.3
	10	62.2	32.2	4.6	1.0
M3-26RAP	0	63.1	27.3	4.5	5.1
	2	62.2	28.4	4.7	4.7
	5	61.8	28.6	5.1	4.5
	7	61.3	28.7	5.9	4.1
	10	60.8	29.0	6.3	3.9
M4-SMA	0	67.7	23.8	3.0	5.5
	2	65.9	24.7	4.2	5.2
	5	65.4	24.9	4.5	5.2
	7	64.3	25.9	4.9	4.9
	10	64.1	26.1	5.1	4.7

Recovered asphalt binder type	Aging level (days)	Maltenes% (<3K)	Asphaltenes% (3-19K)	MMW% (19-45K)	HMW% (>45K)
M5-18RAP	0	66.9	28.3	3.8	1.0
	2	66.2	28.3	4.1	1.0
	5	65.5	28.7	4.7	0.9
	7	65.2	28.9	4.8	0.8
	10	64.7	29.2	4.9	0.7
M6-15RAP	0	68.4	27.5	3.3	0.8
	2	66.8	28.0	4.0	1.2
	5	65.3	28.4	4.5	1.7
	7	63.8	28.6	5.1	2.5
	10	60.8	29.0	6.3	3.9
M7-15RAP	0	69.9	26.4	3.2	0.5
	2	69.0	26.9	3.3	0.8
	5	67.8	27.5	3.6	1.0
	7	67.6	27.8	3.7	0.9
	10	67.4	28.0	3.7	1.0
M8-15RAP	0	70.4	28.2	1.4	0.0
	2	68.5	29.4	2.0	0.1
	5	66.4	30.7	2.5	0.3
	7	66.3	30.2	2.8	0.7
	10	66.4	29.4	3.3	0.9

Note: High molecular weight = HMW; Medium molecular weight = MMW.

Superpave Performance Grading

Figure 6 shows the high PG (HPG) results for the asphalt binders. HPG increased with aging within each mixture type. There was no significant difference in the HPG of the 5- and 7-day aged samples. Further, recovered asphalt binders from M3 showed the highest HPG values indicating the highest level of oxidation among the samples.

Figure 6. High PG Results

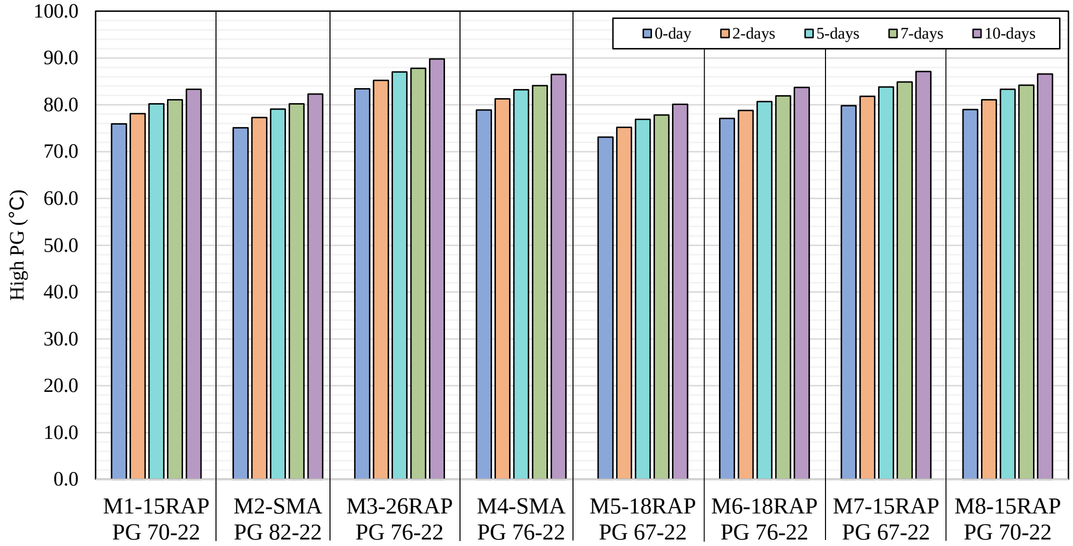

Figure 7 presents ΔT_c results from the BBR test for the asphalt binders. With increasing aging level, ΔT_c became more negative for all asphalt binder types. This observation is consistent with what is reported in the literature [2]. More negative ΔT_c values represent decreased stress relaxation capacity. Asphalt binders with aging levels greater than 2 days yielded negative ΔT_c values, indicating asphalt binders were m-controlled ($T_m > T_s$). It is noted that the asphalt binder recovered from M3 possessed the lowest ΔT_c value at the 10-day aging level, indicating the lowest ductility and potential to relax stress under loading. The relatively lower ΔT_c values for M3 can be attributed to the high RAP content (26%, RBR) used in the mixture. Asphalt binder recovered from M4 showed the highest ΔTc values at 5-, 7-, and 10-day aging levels, which can be attributed to the use of the polymer-modified asphalt binder and no RAP addition.

An aging difference (AD) was defined as the absolute value of the difference between ΔT_c values at 0-day and 10-day aging levels. Higher AD values show higher susceptibility to aging. Asphalt binder recovered from M4 showed the lowest AD value among all asphalt mixtures, suggesting the lowest susceptibility to aging, which is consistent with the observation that the asphalt binder from M4 exhibited the highest ΔTc values at 5-, 7-, and 10-day aging levels compared to other mixtures. Similarly, FTIR test results indicated that M4 had the lowest susceptibility to aging. Further, M4 had the highest effective asphalt binder content and was prepared with a polymer-modified asphalt binder type as the base binder. M3 and M8 (especially M3), on the other hand, showed the highest aging susceptibility to aging. Both mixes possessed a relatively low effective asphalt binder content, as well as a high RAP content, which were effective in increasing the aging susceptibility of the asphalt mixture.

Figure 7. ΔTc Results

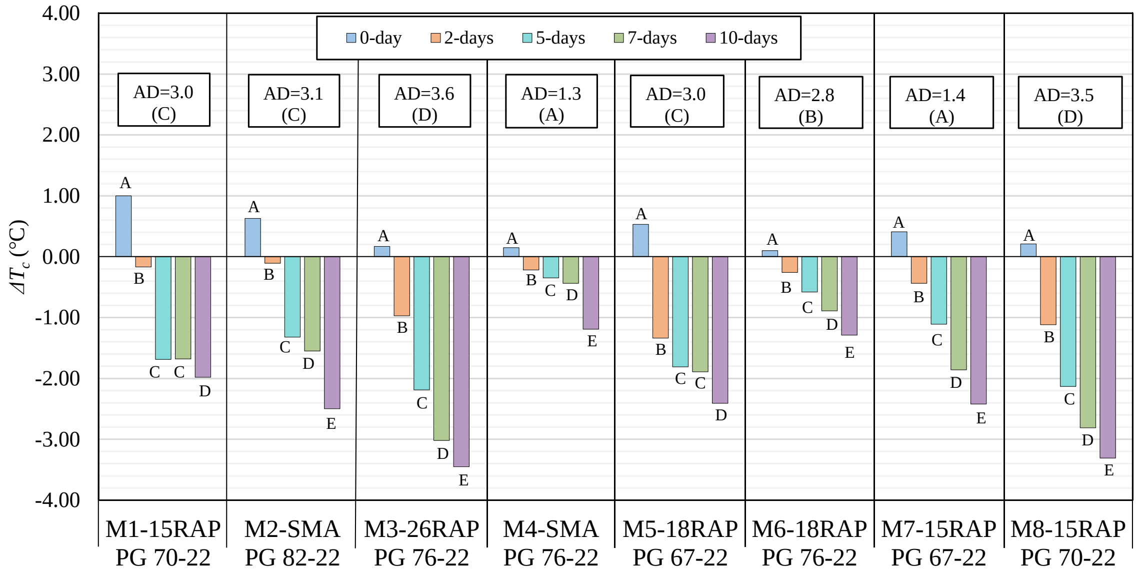

Frequency Sweep Test

Figure 8 presents the G-R values of the studied asphalt binders. The effects of aging intensities on stiffness and ductility properties were quantified using the Glower-Rowe (G-R) parameter. In general, G-R value of each asphalt binder increases with aging. However, recovered asphalt binders from M1, M2, and M5 showed similar G-R values at 5- and 7-day aging levels. While asphalt binders at the 10-day aging level showed significantly higher G-R values as compared to the 7-day aging level, suggesting the decreased ductility of the samples due to oxidative aging.

The rate of change in the G-R parameter with aging was quantified using an aging index (AI), defined as the ratio of G-R value of a 10-day aged sample to G-R value of a 0-day aged sample. Lower AI values indicate a lower rate of aging as measured by G-R parameter. Asphalt binders recovered from M4 and M7 showed the lowest AI values, suggesting the lowest rate of aging. Further, asphalt binder recovered from M3 yielded the highest rate of aging with respect to G-R parameter. These observations were consistent with BBR test results.

Figure 8. Frequency Sweep Test Results

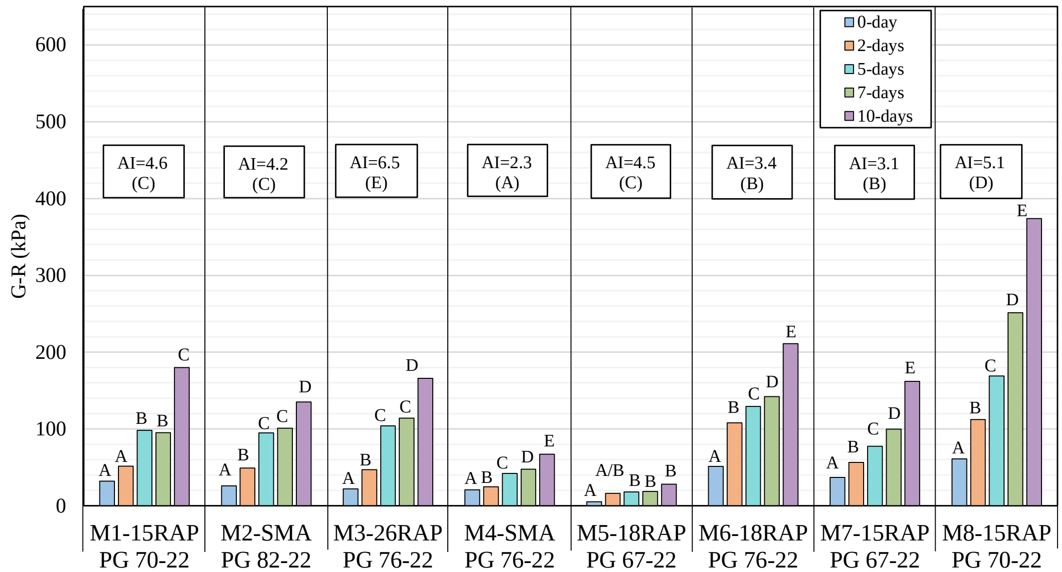

Linear Amplitude Sweep (LAS) Test Results

Figure 9 shows the LAS test results. The A_{LAS} parameter was used to evaluate fatigue performance of asphalt binders at different aging levels. Higher A_{LAS} values represent better fatigue cracking resistant materials [67]. Statistical ranking of the results showed that, in general, the fatigue cracking resistance of asphalt binders decreased with increasing aging levels. Asphalt binders recovered from mixes at 0-day aging level yielded the highest fatigue cracking resistance. Further, the ratio of A_{LAS} parameter at 10-day aging level to 0-day aging level was defined as the aging index (AI) for the analysis (see Figure 9). Lower AI values represent more aging and crack resistant asphalt binders. Asphalt binders recovered from M3 and M4 showed relatively low AI values among the samples. It is noted that these mixtures contained SBS modified asphalt binder, which is known to be resistant against aging and cracking [70, 71]. Further, M2 showed the relatively high AI value and high A_{LAS} value. The high AI may be attributed to presence of crumb rubber modified (CRM) asphalt binder (PG 82-22) in M2. However, the presence of CRM did not improve aging resistance in this mix. It is noted that these observations were similar to results of FTIR and GPC tests.

Figure 9. LAS Test Results

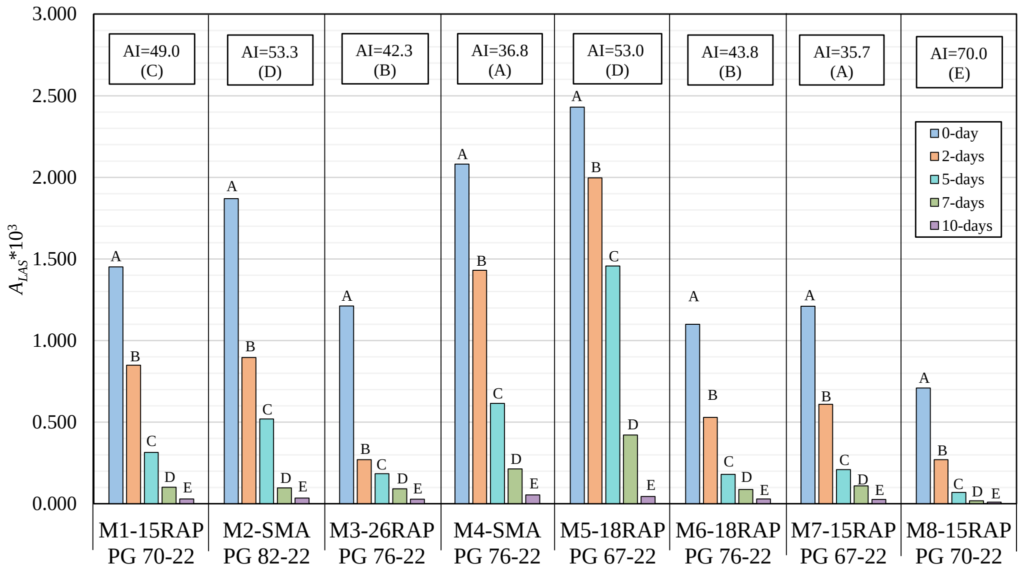

Multiple Stress Creep Recovery (MSCR) Test

Figure 10 presents MSCR test results, percent recovery (*%R*) and non-recoverable creep compliance ($J_{nr,\ 3.2}$), of recovered asphalt binders for the stress level of 3.2 kPa at 64°C. It was found that J_{nr} decreased with increasing aging level, while *%R* increased with aging. These observations can be attributed to the decreased non-recoverable strain due to oxidative aging. Additionally, except for M5 (0- and 2-days) and M8 (10-days) samples, all other recovered asphalt binders showed $J_{nr,\ 3.2}$<0.5 1/kPa, which depicts rut-resistant asphalt binders for extreme traffic level (>30million ESAL + standard traffic).

Figure 10. MSCR Test Results

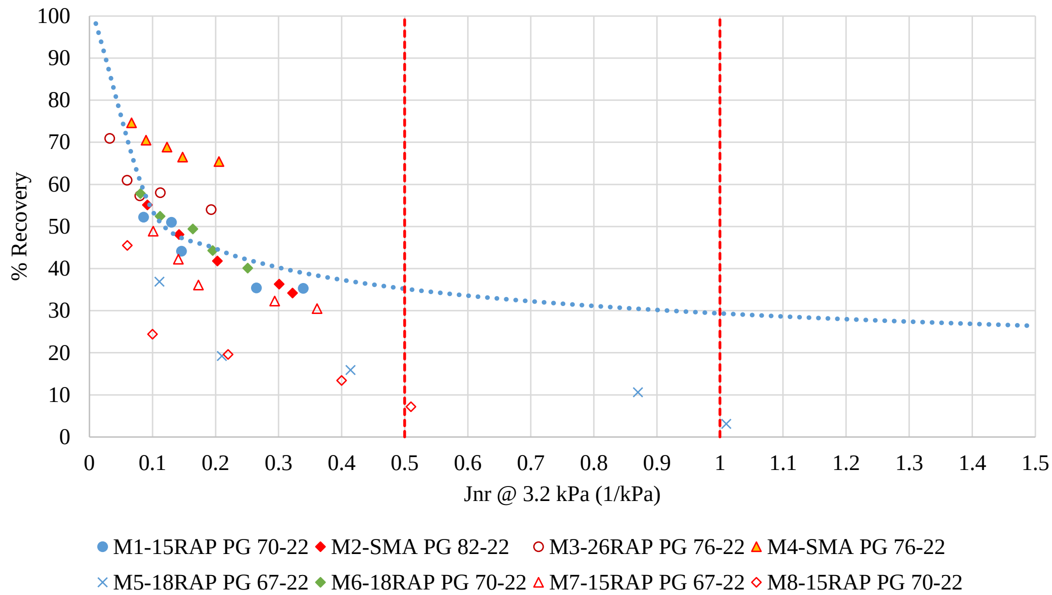

Asphalt Mixture Testing

SCB Test

Figure 11 presents the SCB test results for the asphalt mixtures at different aging levels. Plant-produced asphalt mixtures with no further aging were designated as 0-day aged mixtures. In general, SCB *Jc* values decreased with an increase in aging level. Statistical analysis of the results in Figure 11 indicates that asphalt mixtures at 0-day aging level showed the highest SCB *Jc* parameter. There was no statistically significant difference in the fracture resistance of asphalt mixtures at 2- and 5-day aging levels. Further, the 10-day aging level yielded asphalt mixtures with significantly lower SCB *Jc* compared to other aging levels. M5 had relatively low SCB *Jc* values compared to the other mixtures. It is noted that these mixtures included unmodified asphalt binder (PG 67-22), which made the asphalt mixture less crack resistant.

With the available SCB *Jc* data encompassing both 0 days and 5 days of aging, it becomes possible to derive a scaling factor (see Figure 11b). This scaling factor facilitates the projection of SCB *Jc* values at 5 days aging from those observed at 0 days aging (SCB *Jc* at 5 days aging = SCB *Jc* at 0 days aging – 0.2). However, it is crucial to acknowledge that this relationship between SCB *Jc* values at 5 days aging and those at 0 days aging is established using a limited dataset. The accuracy of such projections could significantly benefit from an expansion of the database, involving more data points to enhance precision and reliability.

Figure 11. SCB Test Results

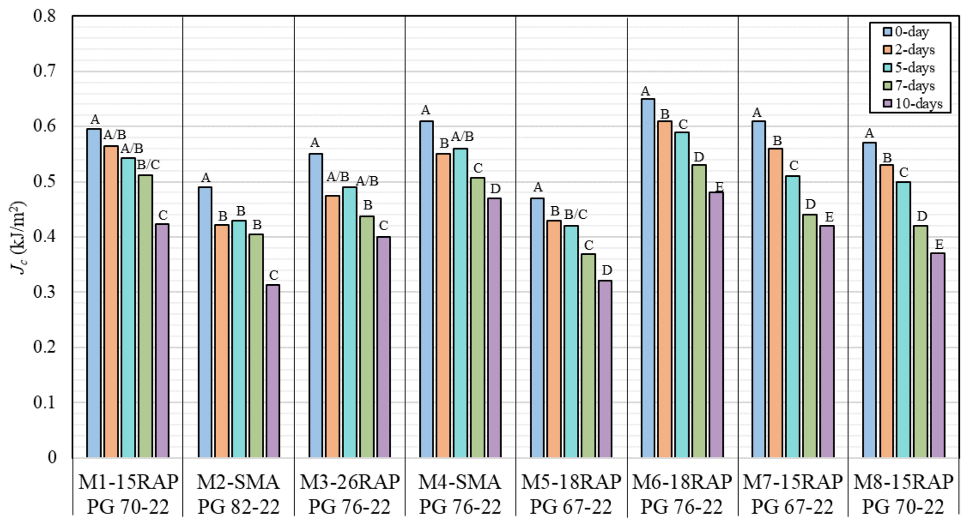

(a)

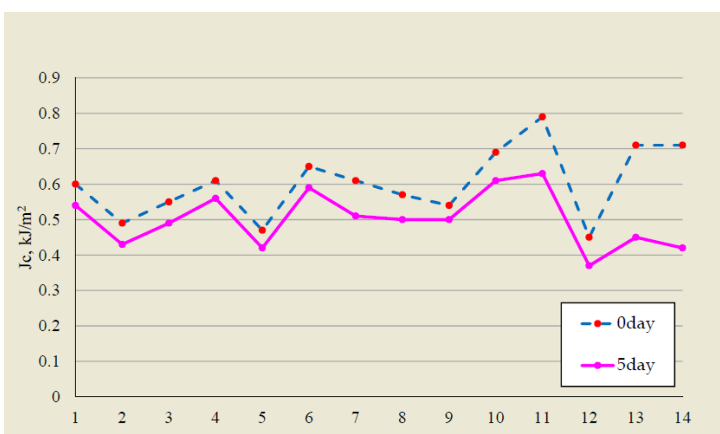

Mix No.			
	0day	5day	Diff
Mix-1	0.6	0.54	0.06
Mix-2	0.49	0.43	0.06
Mix-3	0.55	0.49	0.06
Mix-4	0.61	0.56	0.05
Mix-5	0.47	0.42	0.05
Mix-6	0.65	0.59	0.06
Mix-7	0.61	0.51	0.1
Mix-8	0.57	0.5	0.07
Mix-9	0.54	0.5	0.04
Mix-10	0.69	0.61	0.08
Mix-11	0.79	0.63	0.16
Mix-12	0.45	0.37	0.08
Mix-13	0.71	0.45	0.26
Mix-14	0.71	0.42	0.29
MAX	0.79	0.63	
MIN	0.45	0.37	
AVG	0.603	0.501	0.101
STD	0.1	0.078	

(b)

Comparative Analysis of the Test Results

In order to determine the strength and direction of the correlation between variables, Spearman's rank correlation coefficient (ρ) was used, Equation (19). Spearman's rank correlation coefficient (ρ) is a commonly used parameter to assess rank correlation between variables and ranges from -1 to +1 [72]. The advantage of ρ over other correlation coefficients (i.e., Pearson correlation coefficient and R^2) is that it can be used when the data points are not normally distributed. Spearman's rank correlation is also useful when a non-linear relationship exists between variables [73]. A value of $\rho = 0$ indicates that there is no correlation between two variables, and the correlation becomes stronger as the absolute value of ρ increases. To interpret the correlation coefficient values, the following limits were used based on the existing literature [74, 75]:

$|\rho| < 0.10$: negligible correlation;
$0.11 < |\rho| < 0.39$: weak correlation;
$0.40 < |\rho| < 0.69$: moderate correlation;
$0.70 < |\rho| < 0.89$: strong correlation; and
$0.90 < |\rho| < 1.00$: very strong correlation.

$$\rho = \frac{\sum_{i=1}^{n}(x_i-\bar{x})(y_i-\bar{y})}{\sqrt{[\sum_{i=1}^{n}(x_i-\bar{x})^2][\sum_{i=1}^{n}(y_i-\bar{y})^2]}} \tag{19}$$

Where, ρ is the Spearman's rank correlation coefficient; x_i and y_i are the rank variables for each parameter; and $\bar{x}$ and $\bar{y}$ are the average of rank variables for each parameter.

Table 4 shows pairwise correlation results for all possible combinations of the evaluated parameters. A t-test was performed to determine whether the correlation coefficients are statistically significant. The null hypothesis for the test was that the correlation coefficient is zero. If the p-value is lower than 0.05, it means that the correlation coefficient is statistically significant. Table 4 shows the Spearman's correlation coefficient on a scale of -0.8 to 0.8.

Based on the result of the correlation analysis, pairwise correlation between asphalt binder chemical parameters (*CI* and *%As*) and asphalt binder rheological parameters (ΔT_c and A_{LAS}) was significantly strong, as indicated by $\rho > 0.75$ and p-value < 0.0001. The strong correlations suggest that the microstructural and molecular changes from increasing the asphaltenes and carbonyl index are the primary cause of the loss in the relaxation capabilities of the asphalt binder (ΔT_c) and decreasing fatigue tolerance of the asphalt binder (A_{LAS}).

A strong correlation was also observed between *%As* and *CI*, which indicates that asphalt binders with higher asphaltene contents are expected to yield higher *CI* values because of oxidative aging. Moderate correlations were evident between G-R and *CI*, ΔT_c, and *%As*. Further, weak correlation was observed between SCB *Jc* and G-R. The weak correlation between SCB *Jc* and G-R is because these tests evaluate asphalt mixture and asphalt binder properties at different performance temperatures (i.e., 25°C and 15°C) and are not expected to be correlated.

As ΔT_c illustrates the ductility and stress relaxation capability of the asphalt binder at low temperatures, it is still beneficial to explore the correlation between the ductility of asphalt binder at low temperatures and the fracture resistance of asphalt mixture at intermediate temperatures. Strong correlation ($\rho = 0.79$) was observed between SCB *Jc* and ΔT_c parameters, suggesting that the stress relaxation capabilities of asphalt binder may be related to fracture resistance of asphalt mixture. Further, moderate correlations were observed between asphalt mixture SCB *Jc* parameter and asphalt binder chemical and rheological parameters (A_{LAS}, *CI*, and *%As*,), suggesting a moderate association between the molecular structure and rheological characteristics of asphalt binder, as well as the fracture properties of asphalt mixture.

Table 4. Pairwise Correlation Analysis

Parameters		ρ	p-value
%As	A_{LAS}	**-0.8149**	<.0001
A_{LAS}	CI	**-0.8078**	<.0001
%As	ΔT_c	**-0.7874**	<.0001
A_{LAS}	G-R	**-0.7809**	<.0001
CI	ΔT_c	**-0.7500**	<.0001
CI	SCB *Jc*	-0.5919	0.0018
%As	SCB *Jc*	-0.5144	0.0085
ΔT_c	G-R	-0.4469	0.0251
G-R	SCB *Jc*	-0.3324	0.1045
%As	G-R	0.4619	0.0201
CI	G-R	0.4723	0.0171
A_{LAS}	SCB *Jc*	0.5629	0.0034

Parameters		ρ	p-value
A_{LAS}	ΔT_c	0.6921	0.0001
%As	CI	**0.7431**	<.0001
ΔT_c	SCB *Jc*	**0.7951**	<.0001

Note: ΔT_c = low temperature parameter from BBR test; G-R = Glower-Row parameter; SCB *Jc* = critical strain energy release rate; *%As* = percent asphaltenes from GPC test; CI = carbonyl index from FTIR test; A_{LAS} = fatigue parameter from LAS test.

Database Used for the ANN Model Development

In order to develop the artificial neural network (ANN) model, a database including 40 asphalt mixtures at different aging levels (i.e., 0-, 2-, 5-, 7-, and 10-day) was used. The asphalt mixtures encompass a range of base binder types (unmodified and polymer modified), various recycled binder ratios (RBR), and different gradations. 104 data points were used to select the significant parameters in determining the cracking performance of the asphalt mixtures to be used in the model development. Asphalt mixture compositions are presented in Table 5.

Table 5. Asphalt Mixture Composition

Mixture Number	RBR, %		Asphalt Binder Content, %	PG of Base Asphalt Binder	Modifier	Aggregate Size	Mixture Source
	RAP	RAS					
1	18	0	5.0	76-22	SBS	(3/4" NMAS)	PL
2	17	0	5.2	76-22	SBS	(1/2" NMAS)	PL
3	25	0	4.8	76-22	SBS	(1/2" NMAS)	PL
4	24	0	5.0	76-22	SBS	(1/2" NMAS)	PL
5	16	0	5.0	76-22	SBS	(3/4" NMAS)	PL
6	0	0	5.3	70-22	SBS	(1/2" NMAS)	LL
7	0	5	5.3	70-22	SBS	(1/2" NMAS)	LL
8	0	5	5.3	70-22	SBS	(1/2" NMAS)	LL
9	0	5	5.3	70-22	SBS	(1/2" NMAS)	LL
10	0	5	5.3	70-22	SBS	(1/2" NMAS)	LL
11	0	5	5.3	70-22	SBS	(1/2" NMAS)	LL
12	0	5	5.3	52-28	None	(1/2" NMAS)	LL
13	15	0	5.3	70-22	SBS	(1/2" NMAS)	LL
14	15	5	5.3	70-22	SBS	(1/2" NMAS)	LL
15	15	5	5.3	70-22	SBS	(1/2" NMAS)	LL
16	15	5	5.3	52-28	None	(1/2" NMAS)	LL

Mixture Number	RBR, %		Asphalt Binder Content, %	PG of Base Asphalt Binder	Modifier	Aggregate Size	Mixture Source
	RAP	RAS					
17	0	0	5.7	76-22	SBS	(1/2" NMAS)	LL
18	0	0	6.3	82-22	CRM	(3/4" NMAS)	LL
19	0	0	6.3	82-22	CRM	(3/4" NMAS)	LL
20	0	0	6.3	82-22	CRM	(3/4" NMAS)	LL
21	0	0	6.3	82-22	CRM	(3/4" NMAS)	LL
22	0	0	6.0	82-22	CRM	(3/4" NMAS)	LL
23	0	0	6.0	82-22	CRM	(3/4" NMAS)	LL
24	0	0	6.3	82-22	CRM	(3/4" NMAS)	LL
25	0	0	6.3	82-22	CRM	(3/4" NMAS)	LL
26	100	0	7.2	76-22	None	(1/2" NMAS)	LL
27	100	0	7.2	70-22	None	(1/2" NMAS)	LL
28	100	0	7.2	76-22	None	(1/2" NMAS)	LL
29	100	0	7.2	70-22	None	(1/2" NMAS)	LL
30	0	0	4.5	67-22	None	(3/4" NMAS)	LL
31	0	0	4.1	67.22	None	(3/4" NMAS)	LL
32	0	0	4.5	67.22	None	(3/4" NMAS)	LL
33	0	0	4.1	70-22	SBS	(3/4" NMAS)	LL
34	0	0	4.5	70-22	SBS	(3/4" NMAS)	LL
35	0	0	4.1	70-22	SBS	(3/4" NMAS)	LL
36	0	0	4.5	76-22	SBS	(3/4" NMAS)	LL
37	0	0	4.1	76-22	SBS	(3/4" NMAS)	LL
38	0	0	4.5	76-22	SBS	(3/4" NMAS)	LL
39	15	0	4.3	70-22	SBS	(1/2" NMAS)	PL
40	0	0	6.0	67-22	None	(1/2" NMAS)	PL

Note: PL = plant produced laboratory compacted; LL = laboratory produced laboratory compacted.

Variable Selection Procedure for Model Development

Table 6 presents 12 variables used for variable selection procedure, including the volumetric properties of asphalt mixture, aging level, and asphalt binder modification level. The purpose of variable selection is to identify parameters that are statistically significant in the prediction of SCB *Jc* fracture parameter.

Table 6. A summary of the Parameters used for Variable Selection Process

Volumetric Properties	Asphalt Binder Properties
%AC (asphalt content)	PM (Polymer Modification Level: 0, 1, and 2) *
%RAS and %RAP	**Aging Level**
P_{be} (effective asphalt binder)	Day (0, 2, 5, 7, or 10)
P200 (%passing no. 200 sieve)	
P4 (%passing no.4 sieve)	
VMA (void in mineral aggregate)	
VFA (void filled with asphalt)	
SA (surface area, m^2)	
FT (film thickness, µm)	
DB (dust to binder ratio)	

Note: RAS = recycled asphalt shingle; RAP = reclaimed asphalt pavement;
* 0 = unmodified binder; 1 = moderately modified binder; 2 = highly modified binder.

Stepwise Regression Analysis

In order to find the significant variables to predict the SCB *Jc* of asphalt mixtures, a stepwise regression analysis was performed. Stepwise regression is a method for building a model by successively adding or removing independent variables based on the F-statistics of the estimated coefficients. The process starts with a one-variable model, which has the lowest F-statistics. A threshold of 0.1 was considered, as the F-statistic for a variable can enter the model (F-to-enter < 0.1). For the two-variable model, the variable with the lowest F-statistic enters the model, while the variable with an F-statistic higher than 0.1 leaves the model (F-to-remove). This process continues until the point at which there is no significant variable to enter the model. Table 7 presents the result of the stepwise regression analysis. It was shown that six independent variables, including day (aging level), P_{be}, PM, FT, SA, and P4, were determined to be significant variables in predicting the SCB *Jc* of asphalt mixtures.

Table 7. Stepwise Regression Result

Step	Parameter	Action	"Sig Prob"	R^2	Cp	p	AIC	BIC
1	SA	Entered	0.0000	0.3210	139.76	2	-98.142	-90.48
2	Day	Entered	0.0000	0.5086	75.789	3	-129.28	-119.15
3	PM	Entered	0.0000	0.6105	41.936	4	-151.03	-138.47
4	P4	Entered	0.0000	0.6769	20.607	5	-168.01	-153.08
5	P_{be}	Entered	0.0149	0.6961	15.839	6	-172.03	-154.77
6	SA	Removed	0.7551	0.6958	13.947	5	-174.23	-159.3
7	FT	Entered	0.0226	0.7118	10.339	6	-177.47	-160.21

Step	Parameter	Action	"Sig Prob"	R^2	Cp	p	AIC	BIC
8	SA	Entered	0.0187	0.7280	6.6362	7	-181.09	-161.54
9	RAS	Entered	0.0772	0.7369	5.5271	8	-182.09	-160.31
10	All	Removed	.	0.0000	250.61	1	-60.395	-55.246
11	SA	Entered	0.0000	0.3210	139.76	2	-98.142	-90.48
12	Day	Entered	0.0000	0.5086	75.789	3	-129.28	-119.15
13	PM	Entered	0.0000	0.6105	41.936	4	-151.03	-138.47
14	P4	Entered	0.0000	0.6769	20.607	5	-168.01	-153.08
15	P_{be}	Entered	0.0149	0.6961	15.839	6	-172.03	-154.77
16	SA	Removed	0.7551	0.6958	13.947	5	-174.23	-159.3
17	FT	Entered	0.0226	0.7118	10.339	6	-177.47	-160.21
18	SA	Entered	0.0187	0.7280	6.6362	7	-181.09	-161.54

Note: SA = surface area; PM = polymer modification level; P4 = percent passing from sieve #4; P_{be} = effective asphalt binder; FT = film thickness; RAS = recycled asphalt shingle; Cp = Mallows's Cp; p = total number of parameters in the model; AIC = Akaike information criterion; BIC = Bayesian information criterion.

Multicollinearity Assessment

Multicollinearity is defined as a correlation between independent variables in a multiple regression when more than two independent variables are involved. When multicollinearity increases, the estimated coefficients of the regression model become unstable, and the standard error inflates. Therefore, it is important to evaluate the multicollinearity between independent variables.

Figure 12 presents a summary of the test results in the form of a scatter plot matrix. This type of data presentation is useful when more than two independent variables are involved in the analysis [76]. It could also be helpful to visually capture the multicollinearity between independent variables [77]. The scattered plots are symmetric with respect to the diagonal, which are presenting the variables. Each individual plot is recognized by the x- and y-axes, which are positioned on the bottom and left side of the scattered plot, respectively. If the data points are concentrated around the diagonal, it means there is a high multicollinearity between independent variables [78]. Based on Figure 12, it was visually observed that there was no, or slight, multicollinearity between independent variables. A decreasing trend in the *Jc* of asphalt mixtures with increasing aging duration was observed. This observation implies the effect of progressive oxidative aging on the cracking resistance of asphalt mixtures. Additionally, it was observed that increasing the asphalt film thickness (FT) caused the *Jc* to increase as well. This observation indicates that asphalt mixtures with a higher asphalt binder film thickness will have higher cracking resistance. Further, asphalt mixtures with higher effective asphalt binder contents showed higher *Jc* values, indicating the effect of increased asphalt binder content on the cracking resistance of asphalt mixtures. In addition, asphalt mixtures prepared with polymer-modified asphalt binders showed higher cracking resistance than those prepared with unmodified asphalt binders.

Figure 12. Relationships between Significant Variables

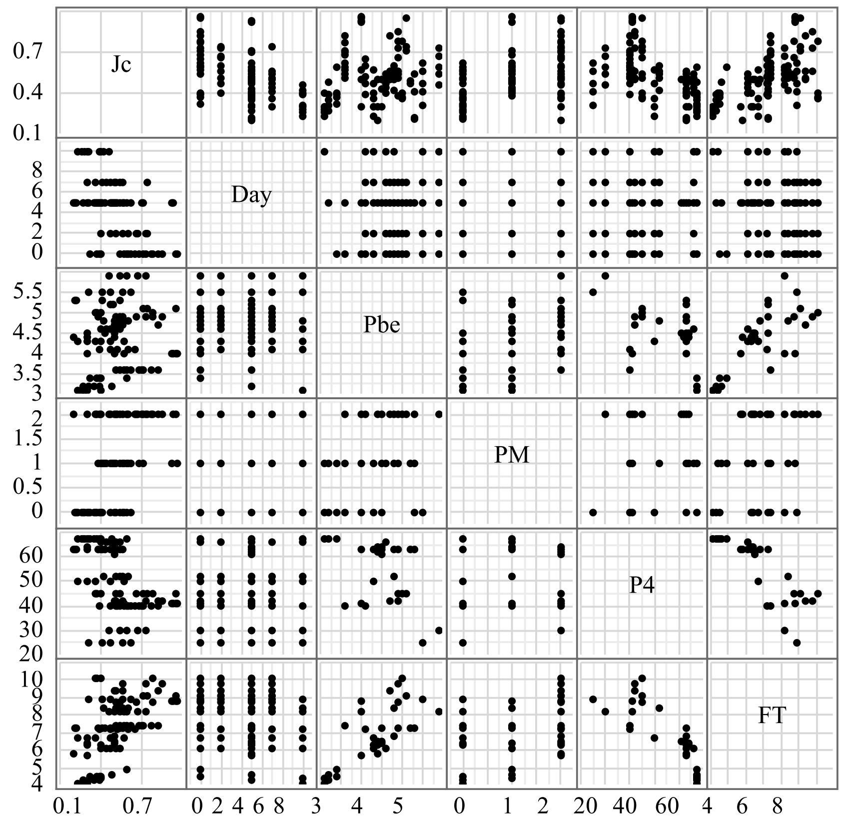

In order to quantify multicollinearity between variables, variance inflation factor (VIF) should be determined. VIF is a common parameter used to assess multicollinearity between variables. Equation (20) shows how this parameter is calculated using a linear regression between independent variables. VIF of 10, or R^2 of 0.90, are considered as threshold values [79-81]. VIF values greater than 10, or R^2 values higher than 0.90, are indicative of multicollinearity between variables.

$$VIF = \frac{1}{1-R^2} \tag{20}$$

Where,
VIF is variance inflation factor; and
R^2 is the coefficient of determination between variables.

Table 8 shows the results of the multicollinearity analysis. Except for SA, all other parameters exhibited VIF and R^2 values less than 10 and 0.90, respectively, which shows there was no multicollinearity between these independent variables.

Table 8. Results of Multicollinearity Analysis

Term	Estimate	Std Error	t Ratio	Prob>|t|	VIF
Intercept	0.566	0.168751	3.36	0.0011	-
Day	-0.024	0.003185	-7.55	<.0001	1.1
FT	0.0631	0.019005	3.32	0.0013	6.2
SA	0.0515	0.021979	2.34	0.0212	**10.9**
P4	-0.0053	0.001221	-4.37	<.0001	2.8
PM	0.1793	0.028489	6.29	<.0001	1.9
P_{be}	-0.1291	0.030998	-4.17	<.0001	6.2

Note: R^2 = coefficient of determination; VIF = variance inflation factor; P_{be} = effective asphalt binder content; FT = film thickness; SA = surface area; P4 = passing from sieve #4; PM = polymer modification level.

ANN Approach and Model Development

ANN Structure

The ANN structure consists of neurons (nodes), links (arrows), input layer, hidden layers, and output layer, as shown in Figure 13. Each neuron in the input layer introduces its value to all the neurons in a hidden layer through links with associated weights. Each neuron in the hidden layer takes the sum of its weighted inputs and applies a non-linear activation function (i.e., transfer function) on the sum. The result of the function then becomes an input for the next step. As the final step, the output neuron takes the sum of the weighted inputs from the previous layer and applies the activation function to the weighted sum. The error is then calculated based on the difference between the predicted and measured output. Equation (21) presents the relationship between inputs, output, weights, and bias. The activation function used in this study was a hyperbolic tangent function presented in Equation (22).

Figure 13. Typical ANN Structure

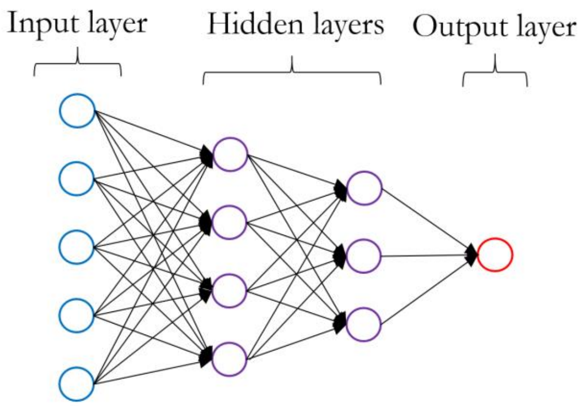

$$J_{c,p} = g\left\{B_0 + \sum_{k=1}^{l} W_k^0 g\left[\sum_{j=1}^{m} W_{jk}^2 g\left(B_{hj}^1 + \sum_{i=1}^{n} W_{ij}^1 X_i\right) + B_{hk}^2\right]\right\} \quad (21)$$

Where,

$J_{c,p}$ is the predicted output,

l is the number of independent variables,

m and n are the number of neurons in the second and first hidden layers, respectively,

g is the nonlinear activation function (tanh),

B_0, B_{hk}^2, B_{hj}^1, are the bias for the output, second hidden layer, and first hidden layer, respectively,

W_k^0, W_{jk}^2, W_{ij}^1 are the weight of the links for the output, second hidden layer, and first hidden layer, respectively, and

X_i is i^{th} input variable.

$$\tanh(x) = \frac{e^x - e^{-x}}{e^x + e^{-x}} \quad (22)$$

The learning capability of the network is obtained by adjusting the value and sign of the weights according to the error through the backpropagation process. The gradient descent method was used to adjust the weight values. In this method, the weight signs and values were adjusted to minimize the error. The iterative process continued until the error was smaller than the threshold value [82]. The weights and biases were updated with respect to the mechanism presented in Equations (23) and (24). This process started with assigning initial values to weights and biases. Then, the first derivative of the error with respect to each weight was determined. The weights were adjusted depending on the sign and magnitude of the derivative. If the derivatives were negative, the weight values were increased by a specific rate, learning rate (α). This process continued until the difference between the predicted and measured output was minimal.

$$W_i = W_i^0 \pm \alpha \frac{\partial E(W_i)}{\partial W_i} \tag{23}$$

$$B_i = B_i^0 \pm \alpha \frac{\partial E(B_i)}{\partial B_i} \tag{24}$$

Where,
W_i and B_i are the updated weight and bias,
W_i^0 and B_i^0 are the initial weight and bias,
α is the learning rate, and
$E(W_i)$ and $E(B_i)$ are the error as a function of weight and bias, respectively.

Model Development

A mathematical software [83] was used to develop the ANN model. Figure 14 shows the step-by-step procedure for the development of the model. 104 data points obtained from laboratory experiments were used for the model development, where 70% of the data points were used for training and 30% for validation of the network. Previous studies suggested that the sample size (i.e., model degree of freedom) should be significantly higher than the number of independent variables [84, 85]. However, some studies recommended that the sample size needs to be at least 10 times of the number of independent variables [86, 87]. In this study, the sample size (104) was approximately 20 times the number of independent variables. In order to reduce data redundancy, all of the data points were normalized using Equation (25).

$$X_{new} = \frac{X - X_{min}}{X_{max} - X_{min}} \tag{25}$$

Figure 14. ANN Model Development Procedure

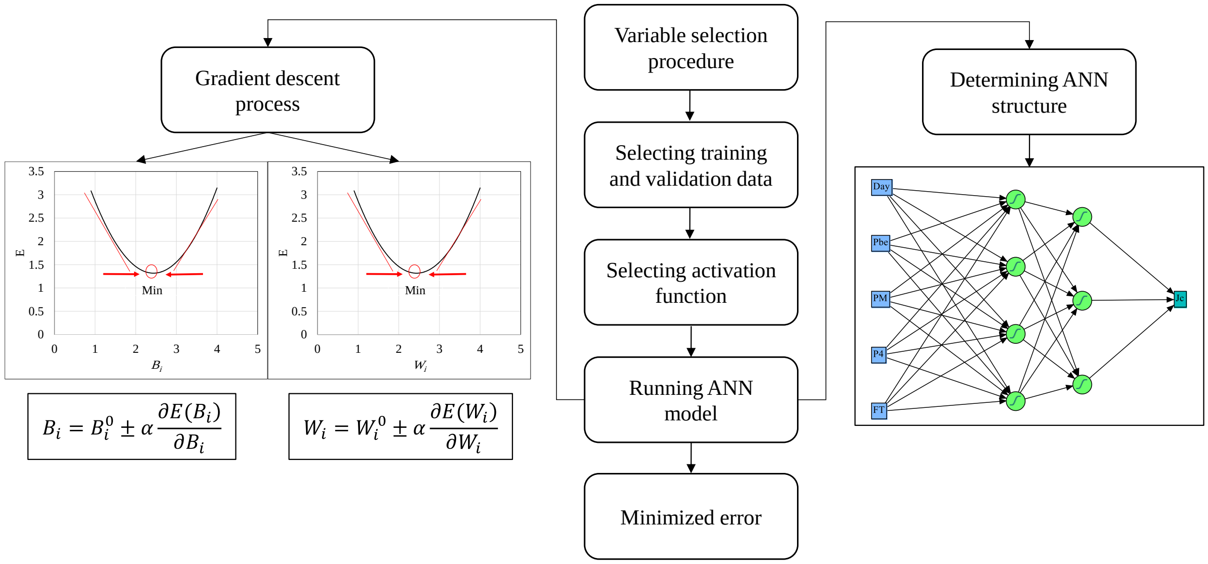

Different network structures were applied to achieve an ANN model with the minimum error, maximum goodness of fit (as measured by R^2), and minimum root mean square error (RMSE) for both training and validation datasets, Equations (26-28). A backpropagation process was performed using the gradient descent procedure to iteratively adjust the weights and minimize the error. A two-hidden layer structure with 4 and 3 neurons at each hidden layer was found to yield the minimum error and maximum goodness of fit. Figure 15 shows the structure of the ANN model that predicts the SCB *Jc* of asphalt mixtures with respect to aging level (day), effective asphalt binder (P_{be}), polymer modification level (PM), percent passing from sieve #4 (P4), and asphalt film thickness (FT).

$$E = \sum_{i=1}^{n} \frac{\left(J_{c,i} - \hat{J}_{c,i}\right)^2}{2} \tag{26}$$

$$R^2 = 1 - \frac{\sum_{i=1}^{n}\left(J_{c,i} - \hat{J}_{c,i}\right)^2}{\sum_{i=1}^{n}\left(J_{c,i} - \bar{J}_{c,i}\right)^2} \tag{27}$$

$$RMSE = \sqrt{\frac{\sum_{i=1}^{n}\left(J_{c,i} - \hat{J}_{c,i}\right)^2}{n}} \tag{28}$$

Where,
E is the error,
R^2 is the coefficient of determination,
$J_{c,i}$ and $\hat{J}_{c,i}$ are the measured and predicted values of the i^{th} output, respectively,
$\bar{J}_{c,i}$ is the average value if the measured outputs,
RMSE is the root mean square error, and
n is the number of data points.

Figure 15. Structure of ANN Model for Predicting Jc

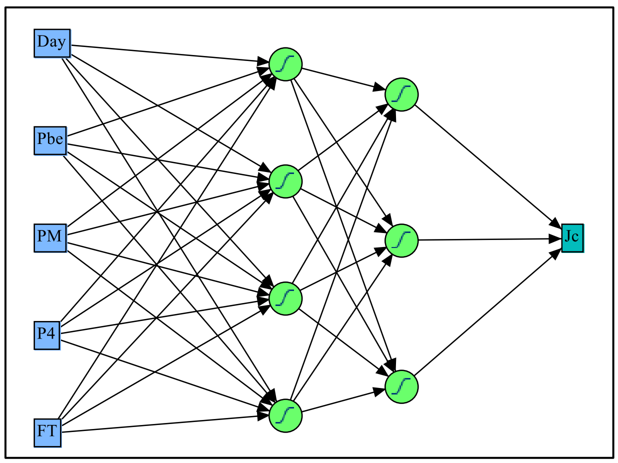

Figure 16(a) presents the relationship between the measured and predicted SCB *Jc* values based on the ANN model with a 95% confidence interval (C.I.) and prediction interval (P.I.). The ANN model was able to predict the SCB *Jc* of asphalt mixtures with an RMSE of 0.042 kJ/m^2 and R^2 of 0.95. The range of measured SCB *Jc* values used for model development was between 0.20 and 0.95 kJ/m^2, which represents a wide range of asphalt mixtures in terms of fracture performance tolerance.

Figure 16(b) illustrates the residual normal quantile versus the predicted *Jc* values. The concentration of the data points around the straight line is an indication of a normal distribution of the residuals.

Figure 16. Training Result (a) Predicted versus Measured SCB Jc, (b) Residual Normal Quantile Plot

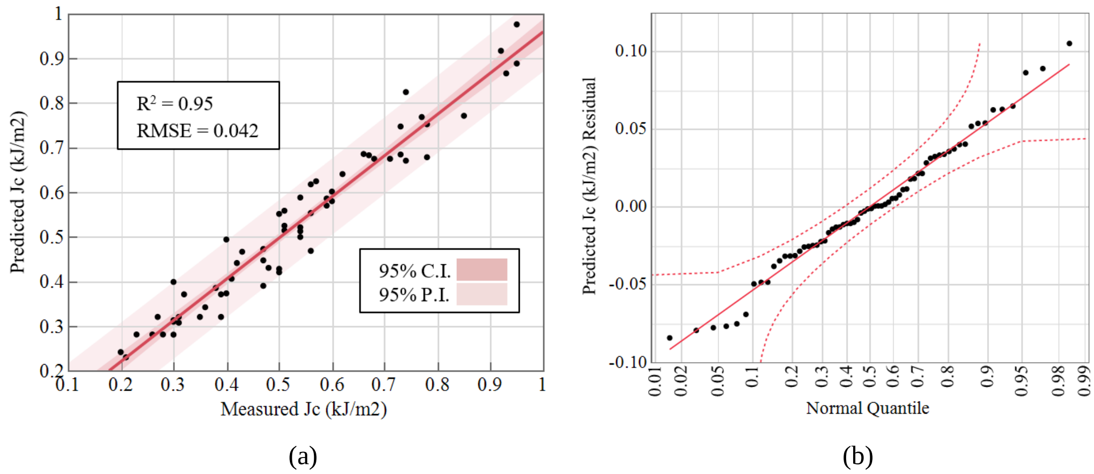

Model Validation

Figure 17 shows the result of model validation for the developed model by comparing the measured and predicted SCB *Jc* values with a 95% confidence and prediction interval. It should be noted that the validation dataset (30% of the data points) was independent of the training dataset. Figure 17(a) shows that the proposed ANN model was validated with an R^2 of 0.92 and RMSE of 0.051 kJ/m^2. The range of SCB *Jc* values used for model validation was between 0.22 and 0.96 kJ/m^2. Figure 17(b) shows the residual normal quantile versus the predicted *Jc* values. As shown in the figure, concentration of the data points around the straight line is an indication of the normal distribution of the residuals.

Figure 17. Validation Result (a) Predicted versus Measured SCB Jc,
(b) Residual Normal Quantile Plot

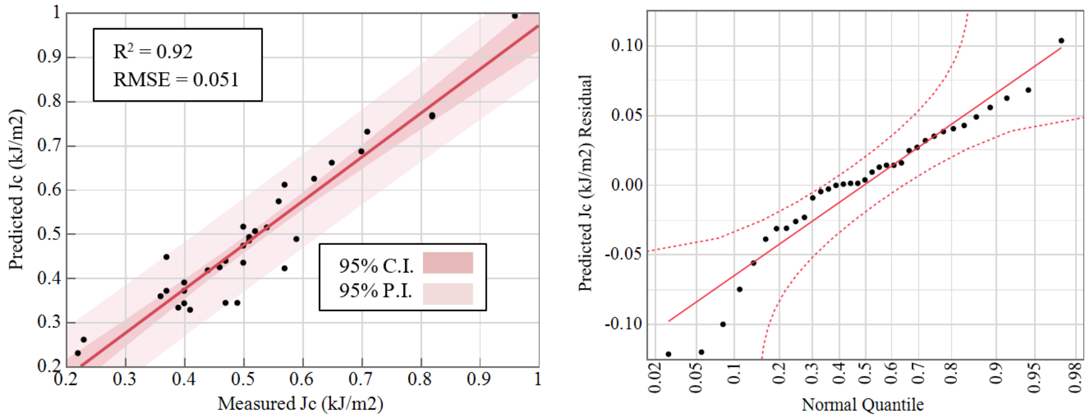

(a) (b)

As mentioned earlier, experimental data for mixtures M9 to M14 (Table 1) that were not used in the development of the ANN model were employed to test and validate the accuracy of the developed predictive model. In Figure 18, the measured and predicted SCB *Jc* values (at 5-days aging) for mixture M9-M14 are compared. The ANN model demonstrates the capability to accurately forecast the long-term aged SCB *Jc* values for hot mix asphalts (HMAs) with an error [i.e., abs (Measured –Predicted)/Measured 100%]

of less than 15%. However, it is important to note that the prediction error for the SMA (M13-SMA) is substantial.

Figure 18. Comparison of Measured and Predicted SCB Jc Values for M9-M14

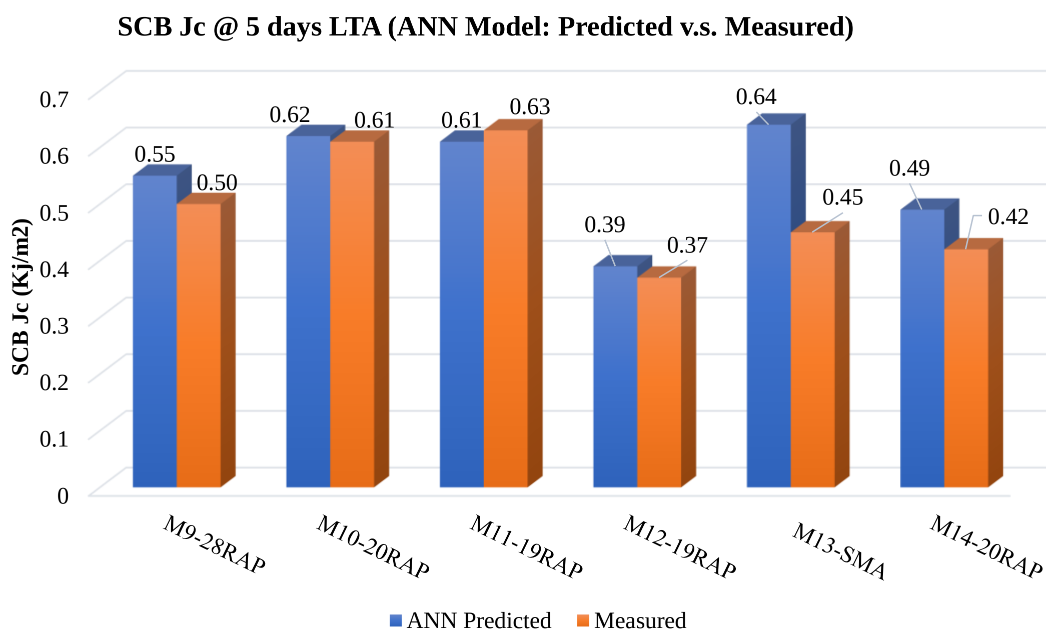

Development of User Interface

A user-friendly interface was developed for applications of the developed ANN model. The model calculates the predicted long-term aged SCB *Jc* values from input variables. The user interface is designed using module PyQt5. This module is a Graphical User Interface (GUI) widgets toolkit for python that is compiled into an executable program. As a stand-alone compiled program, the developed interface is user-friendly. It is also capable of importing or exporting multiple data from/to Excel or csv file format. Figure 19 shows the ANN SCB *Jc* prediction model computer-based interface. The interface contains three parts: a project manager, an interactive table of model inputs, and a report page. The parameter and film thickness can be calculated from mixture design information, and the calculation was automated in the software (Figure 19b). It is worth noting that the Materials Laboratory of the Louisiana Department of Transportation and Development maintains a comprehensive database of materials properties included in this SCB *Jc* prediction model.

Figure 19. The Developed User-Interface for Long-Term Aged SCB Jc Prediction: (a) Project-Info Input, (b) Data Input, and (c) Model Output

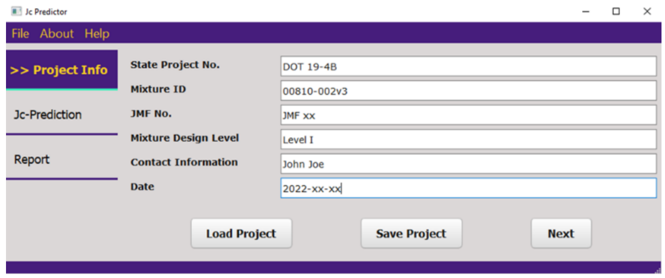

(a)

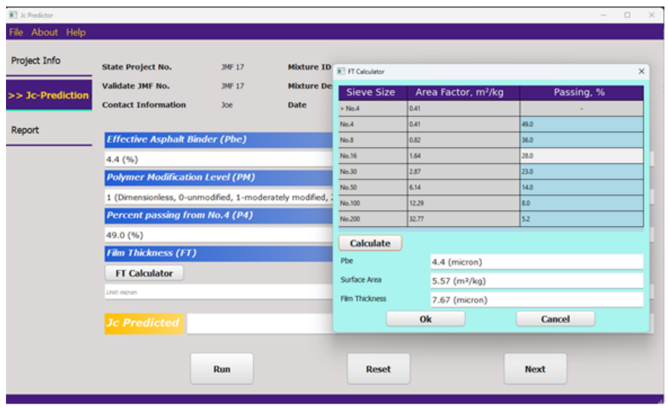

(b)

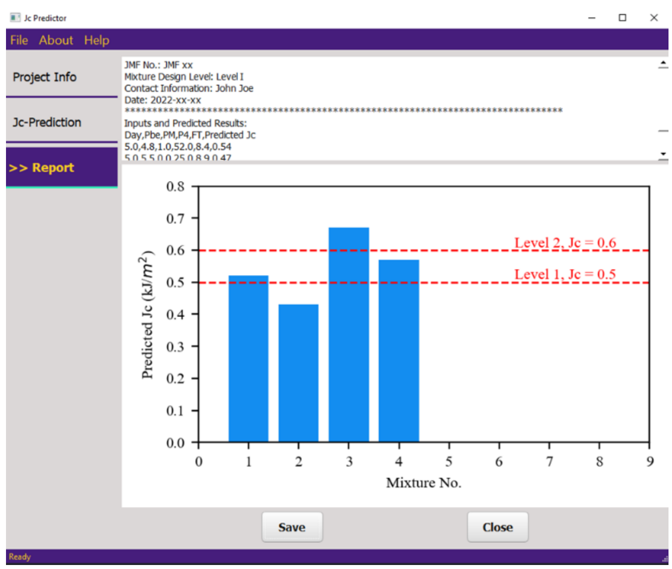

(c)

Conclusions

The objectives of this project were to investigate the effect of laboratory aging on asphalt binders' chemical and rheological properties and asphalt mixtures' cracking resistance, and to develop practical approaches for the prediction of LTA SCB *Jc* for QC/QA testing programs. 14 plant-produced asphalt mixtures from local contractors were acquired and characterized in the LTRC asphalt laboratory. Asphalt binders were extracted and recovered from the compacted mixtures that were aged at different levels. A suite of asphalt binder and asphalt mixture testing methods were employed to characterize the rheological and chemical properties of asphalt binder and cracking resistance of asphalt mixtures. The asphalt binder testing consisted of SARA fractionation, GPC, and FTIR for chemical characterization, as well as Superpave performance grading, frequency sweep, LAS, and MSCR for rheological characterization. The asphalt mixture test method for cracking resistance included the SCB test. Based on the findings, the following conclusions were drawn.

- Chemical tests were effective in capturing incremental aging.
  - GPC analysis revealed that maltene and high-molecular weight components of the asphalt binders reduced with an increase in aging level, while medium-molecular weight and asphaltene components increased due to the oxidative aging.
  - SARA analysis showed that asphaltene content increased with increasing aging durations.
  - FTIR analysis indicated that carbonyl index (*CI*) increased because of oxidative aging.
- Rheological tests were able to capture the effect of oxidative aging.
  - ΔT_c parameter obtained from the BBR test showed larger negative values when aging level increased, which indicates that the stress relaxation capability decreased.
  - G-R parameter obtained from frequency sweep increased with increasing aging levels.
  - A_{LAS} parameter obtained from LAS test decreased with increasing aging duration.

- SCB test was effective in capturing the effect of progressive aging. Cracking resistance of asphalt mixtures in terms of the SCB *Jc* fracture parameter decreased with an increase in aging level.
- SCB *Jc*, A_{LAS}, and FTIR *CI* parameters were consistently able to capture the effect of asphalt binder type (unmodified and polymer modified) on the aging susceptibility of asphalt mixture and asphalt binder.
- Correlation analysis indicated that A_{LAS} had a strong correlation with *CI* and *%As*. SCB *Jc* also showed a strong correlation with ΔT_c and moderate correlation with A_{LAS}. These observations suggest a correspondence between the molecular structure of asphalt binder due to aging and the rheological characteristics of asphalt binder, as well as the fracture properties of asphalt mixture.
- A scaling factor was developed to forecast SCB *Jc* at 5 days 85°C aging from SCB *Jc* at 0 days aging (i.e., plant-produced mixtures).
- Statistical analysis of the test results using stepwise regression method showed that the aging level, P_{be}, P4, FT, and PM parameters were significant in determining the SCB *Jc* of asphalt mixtures.
- The ANN approach using the gradient descent backpropagation process has shown to be effective in predicting the SCB *Jc* of asphalt mixtures. The predictive ANN model was able to accurately predict the fracture performance of asphalt mixtures.
- A user-friendly interface was developed for implementation in the Louisiana DOTD’s asphalt mixture QC/QA programs.

Acronyms, Abbreviations, and Symbols

Term	Description
AASHTO	American Association of State Highway and Transportation Officials
ALF	Accelerated Loading Facility
AMPT	Asphalt Mixture Performance Tester
ANN	artificial neural network
ANOVA	Analysis of Variance
ASTM	American Society of Testing Materials
BBR	Bending Beam Rheometer
BF	beam fatigue
CA	Christensen-Anderson
CAB	crushed aggregate base
cm	centimeter(s)
CoV	coefficient of variation
DMR	dynamic modulus ratio
DOT	Department of Transportation
DOTD	Louisiana Department of Transportation and Development
DSR	dynamic shear rheometer
FHWA	Federal Highway Administration
ft.	foot (feet)
FT	film thickness
FTIR	Fourier transform infrared spectroscopy
GPC	gel permeation chromatography
G-R	Glover-Rowe
HMA	hot-mix asphalt
HMW	high molecular weight
LA	Louisiana
LAS	linear amplitude sweep
LSD	least significant difference
LTA	long-term aging

Term	Description
LTRC	Louisiana Transportation Research Center
LVE	linear viscoelastic
lb.	pound(s)
m	meter(s)
MMS	medium molecular size
MSCR	multiple stress creep recovery
NMAS	nominal maximum aggregate size
PAV	pressure aging vessel
PG	performance grade
PM	polymer modification
QC/QA	quality control/quality assurance
RAP	recycled asphalt pavement
RAS	reclaimed asphalt pavement
RBR	recycled binder ratio
RTFO	rolling thin film oven
SARA	saturates, aromatics, resins, asphaltenes
SCB	semi-circular bend
SMS	small molecular size
S-VECD	simplified viscoelastic continuum damage
TCE	Trichloroethylene
VECD	viscoelastic continuum damage
VMA	voids in the mineral aggregate
WMA	warm-mix asphalt

References

[1] W. S. Mogawer, A. Austerman, R. Roque, S. Underwood, L. Mohammad, and J. Zou, "Ageing and rejuvenators: Evaluating their impact on high RAP asphalt mixtures fatigue cracking characteristics using advanced mechanistic models and testing methods," *Road Materials and Pavement Design*, vol. 16, 2015, pp. 1-28.

[2] W. Cao, P. Barghabany, L. Mohammad, S. B. Cooper III, and S. Balamurugan, "Chemical and rheological evaluation of asphalts incorporating RAP/RAS binders and warm-mix technologies in relation to crack resistance," *Construction and Building Materials*, vol. 198, 2019, pp. 256-268.

[3] J. A. Epps, S. Seeds, and C. A. Monismith, *Recommended Performance-Related Specification for Hot-Mix Asphalt Construction: Results of the WesTrack Project*, vol. 455, Washington, DC: Transportation Research Board, 2002.

[4] M. A. Mull, A. Othman, and L. Mohammad, "Fatigue crack propagation analysis of chemically modified crumb rubber-asphalt mixtures," *Journal of Elastomers and Plastics*, vol. 37, no. 1, 2005, pp. 73-87.

[5] M. Kim, L. N. Mohammad, and M. A. Elseifi, "Characterization of fracture properties of asphalt mixtures as measured by semicircular bend test and indirect tension test," *Transportation Research Record*, no. 2296, 2012, pp. 115-124.

[6] Louisiana Department of Transportation and Development, *Standard Specifications for Road and Bridge Construction*, Louisiana, 2016.

[7] K. Ksaibati and N. E. Butts, *Evaluating the impact of QC/QA programs on asphalt mixture variability*, Department of Civil and Architectural Engineering, University of Wyoming, 2003.

[8] J. C. Petersen, "A review of the fundamentals of asphalt oxidation: Chemical, physicochemical, physical property, and durability relationships," *Transportation Research E-Circular*, no. E-C140, 2009.

[9] C. A. Bell, A. Wieder, and M. J. Fellin, *Laboratory Aging of Asphalt-Aggregate Mixtures Field Validation*, Washington, DC: National Research Council, 1994.

[10] AASHTO R30, *Standard Practice for Mixture Conditioning of Hot-Mix Asphalt (HMA)*, American Association of State Highway and Transportation Officials, 2015.

[11] W. N. Houston, M. Mirza, C. E. Zapata, and S. Raghavendra, "Environmental effects in pavement mix and structural design systems," *NCHRP Project*, 2005, pp. 9-23.

[12] L. N. Mohammad, M. Kim, and H. Challa, *Development of Performance-Based Specifications for Louisiana Asphalt Mixtures*, Louisiana Transportation Research Center, Baton Rouge, Louisiana, 2016.

[13] J. C. Petersen and R. Glaser, "Asphalt oxidation mechanisms and the role of oxidation products on age hardening revisited," *Road Materials and Pavement Design*, vol. 12, no. 4, 2011, pp. 795-819.

[14] C. A. Bell, Y. AbWahab, M. E. Cristi, and D. Sosnovske, *Selection of Laboratory Aging Procedures for Asphalt-Aggregate Mixtures*, Strategic Highway Research Program, Washington, DC: National Research Council, 1994.

[15] Y. R. Kim, C. Castorena, M. D. Elwardany, F. Y. Rad, S. Underwood, A. Gundla, P. Gudipudi, M. J. Farrar, and R. R. Glaser, *Long-Term Aging of Asphalt Mixtures for Performance Testing and Prediction*, Transportation Research Board, 2018.

[16] I. Negulescu, L. Mohammad, W. Daly, C. Abadie, R. Cueto, C. Daranga, and I. Glover, "Chemical and rheological characterization of wet and dry aging of SBS copolymer modified asphalt cements: Laboratory and field evaluation (with discussion)," *Journal of the Association of Asphalt Paving Technologists*, vol. 75, 2006.

[17] D. Newcomb, A. E. Martin, F. Yin, E. Arambula, E. S. Park, A. Chowdhury, R. Brown, C. Rodezno, N. Tran, and E. Coleri, *Short-Term Laboratory Conditioning of Asphalt Mixtures*, Washington, DC: National Research Council, 2015.

[18] P. Kandhal, "Low-temperature ductility in relation to pavement performance," in *Low-Temperature Properties of Bituminous Materials and Compacted Bituminous Paving Mixtures*, ASTM International, 1977.

[19] B. Vallerga and W. Halstead, "Effects of field aging on fundamental properties of paving asphalts," *Highway Research Record*, no. 361, 1971.

[20] C. Glover, R. Davison, C. Domke, Y. Ruan, P. Juristyarini, D. Knorr, and S. Jung, *Development of a New Method for Assessing Asphalt Binder Durability with Field Evaluation*, Federal Highway Administration and Texas Department of Transportation, Report No. FHWA/TX-05/1872-2, 2005.

[21] R. M. Anderson, G. N. King, D. I. Hanson, and P. B. Blankenship, "Evaluation of the relationship between asphalt binder properties and non-load related cracking," *Journal of the Association of Asphalt Paving Technologists*, vol. 80, 2011.

[22] G. Rowe, G. King, and M. Anderson, "The influence of binder rheology on the cracking of asphalt mixes in airport and highway projects," *Journal of Testing and Evaluation*, vol. 42, no. 5, 2014, pp. 1063-1072.

[23] D. W. Christensen and D. A. Anderson, "Interpretation of dynamic mechanical test data for paving grade asphalt cements (with discussion)," *Journal of the Association of Asphalt Paving Technologists*, vol. 61, 1992.

[24] A. Booshehrian, W. S. Mogawer, and R. Bonaquist, "How to construct an asphalt binder master curve and assess the degree of blending between RAP and virgin binders," *Journal of Materials in Civil Engineering*, vol. 25, no. 12, 2012, pp. 1813-1821.

[25] K. P. Chong and M. D. Kuruppu, "New specimen for fracture-toughness determination for rock and other materials," *International Journal of Fracture*, vol. 26, no. 2, 1984, pp. R59-R62.

[26] J. R. Rice, "A path independent integral and the approximate analysis of strain concentration by notches and cracks," *Journal of Applied Mechanics*, vol. 35, 1968, pp. 379-386.

[27] P. C. Paris and F. Erdogan, "A critical analysis of crack propagation laws," *Journal of Basic Engineering ASME*, vol. 85, no. 4, 1963.

[28] R. L. Krans, F. Tolman, and M. F. C. Van de Ven, "Semi-circular bending test: A practical crack growth test using asphalt concrete cores," *RILEM Proceedings*, Chapman & Hall, 1996.

[29] M. A. Mull, A. Othman, and L. Mohammad, "Fatigue crack propagation analysis of chemically modified crumb rubber-asphalt mixtures," *Journal of Elastomers and Plastics*, vol. 37, no. 1, 2005, pp. 73-87.

[30] L. N. Mohammad, Z. Wu, and M. A. Aglan, "Characterization of fracture and fatigue resistance on recycled polymer-modified asphalt pavements," in *Proceedings, 5th International Conference on RILEM*, 2004, pp. 375-382.

[31] Z. Wu, N. L. Mohammad, and L. B. Wang, "Fracture resistance characterization of Superpave asphalt mixtures using the semi-circular bending test," *Journal of ASTM International*, 2005, pp. 1-15.

[32] X. Shu, B. Huang, and D. Vukosavljevic, "Evaluation of cracking resistance of recycled asphalt mixture using semi-circular bending test," *Paving Materials and Pavement Analysis (GSP 203)*, 2010, pp. 58-65.

[33] S. Im, Y. R. Kim, and H. Ban, "Rate and temperature dependent fracture characteristics of asphaltic paving mixtures," *Journal of Testing and Evaluation*, vol. 41, no. 2, 2013, pp. 257-268.

[34] K. P. Biligiri, S. Said, and H. Hakim, "Asphalt mixtures' crack propagation assessment using semi-circular bending tests," *International Journal of Pavement Research and Technology*, vol. 5, no. 4, 2012, pp. 209.

[35] F. T. S. Aragao and Y. R. Kim, "Fracture characterization of bituminous paving mixtures at intermediate service temperatures," *Experimental Mechanics*, vol. 52, no. 9, 2012, pp. 1423-1434.

[36] M. A. Elseifi, L. N. Mohammad, H. Ying, and S. Cooper, "Modeling and evaluation of the cracking resistance of asphalt mixtures using the semi-circular bending test at intermediate temperatures," *Road Materials and Pavement Design*, vol. 13, 2012, pp. 124-139.

[37] L. N. Mohammad, M. Kim, and M. A. Elseifi, "Characterization of asphalt mixture's fracture resistance using the semi-circular bending (SCB) test," in *7th RILEM International Conference on Cracking in Pavements*, 2012, pp. 1-10.

[38] J. C. Petersen, P. M. Harnsberger, and R. E. Robertson, "Factors affecting the kinetics and mechanisms of asphalt oxidation and the relative effects of oxidation products on age hardening," *American Chemical Society Division of Fuel Chemistry Preprints*, vol. 41, no. 4, 1996, pp. 1232-1244.

[39] J. C. Petersen, "Chemical composition of asphalt as related to asphalt durability: State of the art," *Transportation Research Record: Journal of the Transportation Research Board*, vol. 999, 1984, pp. 13-30.

[40] F. J. Nellenstyn, "The constitution of asphalt," *Journal of the Institution of Petroleum Technologists*, vol. 10, 1924, pp. 311-325.

[41] F. J. Nellenstyn, "Relation of the micelle to the medium in asphalt," *Journal of the Institution of Petroleum Technologists*, vol. 14, 1928, pp. 134-138.

[42] L. Loeber, G. Muller, J. Morel, and O. Sutton, "Bitumen in colloid science: A chemical, structural and rheological approach," *Fuel*, vol. 77, no. 13, 1998, pp. 1443-1450.

[43] K. W. Kim, J. L. Burati, and S. N. Amirkhanian, "Relation of HP-GPC profile with mechanical properties of AC mixtures," *Journal of Materials in Civil Engineering*, vol. 5, no. 4, 1993, pp. 447-459.

[44] ASTM D3279-12, "Standard test method for n-heptane insolubles," ASTM International, West Conshohocken, PA, 2012.

[45] ASTM E1252, "Standard practice for general techniques for obtaining spectra for qualitative analysis," ASTM International, West Conshohocken, PA, 2012.

[46] H. Nabizadeh, F. H. Haghshenas, R. Y. Kim, and T. F. Aragao, "Effects of rejuvenators on high-RAP mixtures based on laboratory tests of asphalt concrete (AC) mixtures and fine aggregate matrix (FAM) mixtures," *Construction and Building Materials*, vol. 152, 2017, pp. 65-73.

[47] W. Van den Bergh, *The effect of ageing on the fatigue and healing properties of bituminous mortars*, PhD dissertation, Delft University of Technology, 2011.

[48] B. S. Cooper, L. Negulescu, S. S. Balamurugan, L. N. Mohammad, and H. W. Daly, "Binder comparison and intermediate temperature cracking performance of asphalt mixtures containing RAS," *Road Materials and Pavement Design*, vol. 16, no. S2, 2015, pp. 275-295.

[49] J. Liu, J. Liu, and S. Saboundjian, "Evaluation of cracking susceptibility of Alaskan polymer modified asphalt binders using chemical and rheological indices," Construction and Build. Materials, vol. 271, 2021.

[50] ASTM D6579, "Standard practice for molecular weight averages and molecular weight distribution of hydrocarbon, rosin, and terpene resins by size-exclusion chromatography," ASTM International, West Conshohocken, PA, 2011.

[51] AASHTO T 313-12, "Standard method of test for determining the flexural creep stiffness of asphalt binder using the bending beam rheometer (BBR)," Washington, DC, 2016.

[52] AASHTO R 28-12, "Standard practice for accelerated aging of asphalt binder using a pressurized aging vessel (PAV)," Washington, DC, 2016.

[53] AASHTO M 320-17, "Standard specification for performance-graded asphalt binder," Washington, DC, 2017.

[54] ASTM D7643-16, "Standard practice for determining the continuous grading temperatures and continuous grades for PG graded asphalt binders," ASTM International, West Conshohocken, PA, 2016.

[55] D. Lesueur, M. D. Elwardany, J. P. Planche, D. Christensen, and G. N. King, "Impact of the asphalt binder rheological behavior on the value of the ΔTc parameter," *Construction and Building Materials*, vol. 293, p. 123464, 2021, pp. 1-10.

[56] S. Komaragiri, A. Filonzi, E. Guevara, D. Hazlett, E. Mahmoud, and A. Bhasin, "Examining different alternatives to Delta Tc (ΔTc) as a parameter to screen asphalt binders," *Journal of Testing and Evaluation*, vol. 50, no. 1, pp. 391-400, 2022.

[57] T. Yan, E. Mariette, M. Turos, and M. Marasteanu, "Evaluation of physical hardening and oxidative aging effects on Delta Tc of asphalt binders," *Road Materials and Pavement Design*, vol. 24, no. sup1, pp. 626-639, 2023.

[58] M. Elwardany, J. P. Planche, and G. King, "Universal and practical approach to evaluate asphalt binder resistance to thermally-induced surface damage," *Construction and Building Materials*, vol. 255, p. 119331, 2020, pp. 1-11.

[59] R. Moraes and H. Bahia, "Developing simple binder indices for cracking resistance of asphalt binders at intermediate and low temperatures," *Transportation Research Record*, vol. 2672, no. 28, pp. 311-323, 2018.

[60] Y. Kumbargeri, J. P. Planche, J. J. Adams, M. D. Elwardany, and G. King, "Effect of binder chemistry and related properties on the low-temperature performance parameters of asphalt binders," *Transportation Research Record*, vol. 03611981231155173, 2023, pp. 1-15.

[61] ASTM D7175, "Standard test method for determining the rheological properties of asphalt binder using a dynamic shear rheometer," ASTM International, West Conshohocken, PA, 2015.

[62] A. Cannone Falchetto, K. H. Moon, D. Wang, and H. W. Park, "A modified rheological model for the dynamic modulus of asphalt mixtures," Canadian Journal of Civil Engineering, vol. 48, no. 3, 2021, pp. 328-340.

[63] T. Koudelka, P. Coufalik, J. Fiedler, I. Coufalikova, M. Varaus, and F. Yin, "Rheological evaluation of asphalt blends at multiple rejuvenation and aging cycles," Road Materials and Pavement Design, vol. 20, sup1, 2019, pp. S3-S18.

[64] C. Hintz, R. Velasquez, C. Johnson, and H. Bahia, "Modification and validation of linear amplitude sweep test for binder fatigue specification," *Transportation Research Record: Journal of the Transportation Research Board*, vol. 2207, 2011, pp. 99-106.

[65] F. Safaei, C. Castorena, and Y. R. Kim, "Linking asphalt binder fatigue to asphalt mixture fatigue performance using viscoelastic continuum damage modeling," *Mechanics of Time-Dependent Materials*, vol. 20, no. 3, 2016, pp. 299-323.

[66] C. Wang, C. Castorena, J. Zhang, and Y. R. Kim, "Unified failure criterion for asphalt binder under cyclic fatigue loading," *Road Materials and Pavement Design*, vol. 16, no. sup2, 2015, pp. 125-148.

[67] W. Cao, L. N. Mohammad, and P. Barghabany, "Use of viscoelastic continuum damage theory to correlate fatigue resistance of asphalt binders and mixtures," *International Journal of Geomechanics*, vol. 18, no. 11, 2018, p. 04018151.

[68] W. H. Daly, *Relationship between chemical makeup of binders and engineering performance: A synthesis of highway practice*, Report No. NCHRP Synthesis 511, Transportation Research Board, Washington, DC, 2017.

[69] R. Tarefder and S. Yousefi, "Rheological examination of aging in polymer-modified asphalts," *Journal of Materials in Civil Engineering*, vol. 28, no. 2, 2015, pp. 1-12.

[70] A. Diab, M. Enieb, and D. Singh, "Influence of aging on properties of polymer-modified asphalt," *Construction and Building Materials*, vol. 196, 2018, pp. 54-65.

[71] S. Dziadosz, M. Słowik, F. Niwczyk, and M. Bilski, "Study on styrene-butadiene-styrene modified asphalt binders relaxation at low temperature," Materials, vol. 14, no. 11, 2021, pp. 2888.

[72] B. R. Overholser and K. M. Sowinski, "Biostatistics primer: Part 2," *Nutrition in Clinical Practice*, vol. 23, 2008, pp. 76-84.

[73] D. D. Wackerly, W. Mendenhall III, and R. L. Scheaffer, "Multivariate probability distributions," in *Mathematical Statistics with Applications*, 7th ed. Belmont, CA: Brooks/Cole, 2008, pp. 223-295.

[74] P. Schober, C. Boer, and L. Schwarte, "Correlation coefficients: Appropriate use and interpretation," *Anesthesia & Analgesia*, vol. 126, no. 5, 2018, pp. 1763-1768.

[75] M. M. Mukala, "Statistics corner: A guide to appropriate use of correlation coefficient in medical research," *Malawi Medical Journal*, vol. 24, 2012, pp. 69-71.

[76] A. C. Davison and S. Sardy, "The partial scatterplot matrix," *Journal of Computational and Graphical Statistics*, vol. 9, no. 4, 2012, pp. 750-758.

[77] C. Reumann, P. Filzmoser, R. Garrett, and R. Dutter, *Statistical data analysis explained: Applied environmental statistics with R*. John Wiley & Sons Ltd, 2007.

[78] M. C. Hao, U. Dayal, R. K. Sharma, D. A. Keim, H. Janetzko, and H. Visual, "Analytics of large multidimensional data using variable binned scatter plots," *Proc. SPIE 7530, Visualization and Data Analysis*, 2010, p. 753006.

[79] J. F. Hair, W. C. Black, B. J. Babin, R. E. Anderson, and R. L. Tatham, *Multivariate data analysis*, 6th ed. Upper Saddle River, N.J.: Prentice Hall, 2006.

[80] R. O'Brien, "A caution regarding rules of thumb for variance inflation factors," *Quality and Quantity Journal*, vol. 41, 2007, pp. 673-690.

[81] C. Dormann, J. Elith, S. Bacher, C. Buchmann, G. Carl, G. Carre, J. Marquez, B. Gruber, B. Lafourcade, and P. Leitao, "Collinearity: a review of the methods to deal with it and a simulation study evaluating their performance," *Echography*, vol. 36, no. 1, 2012.

[82] A. P. Plumb, R. C. Row, P. York, and M. Brown, "Optimization of the predictive ability of artificial neural network (ANN) models: A comparison of three ANN programs and four classes of training algorithm," *European Journal of Pharmaceutical*, vol. 25, no. 4-5, 2005, pp. 395-405.

[83] RStudio Team, "RStudio: Integrated development for R," RStudio, PBC, Boston, MA. URL http://rstudio.com/, 2020.

[84] S. Lawrence, C. Lee, and A. Tsoi, "What size neural network gives optimal generalization? Convergence properties of backpropagation," Technical report, Institute for Advanced Computer Studies, University of Maryland, 1996.

[85] B. Liu, Y. Wei, Y. Zhang, and Q. Yang, "Deep neural network for high dimension, low sample size data," *Proceeding of the Twenty-Sixth International Joint Conference on Artificial Intelligence*, 2017.

[86] S. J. Raudys and A. K. Jain, "Small sample size effect in statistical pattern recognition: Recommendations for practitioners," *IEEE Transactions on Machine Intelligence*, vol. 13, no. 3, 1991, pp. 252-264.

[87] T. Kavazoglu and P. M. Mather, "The use of backpropagation artificial neural network in land cover classification," *International Journal of Remote Sensing*, vol. 24, no. 23, 2003, pp. 4907-4938.

Appendix

JMF of Mix 1

Louisiana Department of Transportation and Development
JMF SUPERPAVE ASPHALTIC CONCRETE MIXTURES

Metric/English: E
Plant Code: PS00000630-Coastal Bridge, Inc., LLC - Lafayette
SMM ID: 0
Project No.:
Specs: 2016 | Plant Type: 3-dryer drum | Mix Type: Wearing Course | Mix Use: ML - Wearing | Des.Level: 1
ESAL: 0 | Prod.Rate: 350 | Mix Temp: 300 | Seq No: 175
Adj. Factor: 1.00 | ADT/lane: 450 | Nom.Agg.Size: 0.5 in. | AC Corr Factor: 0.14
Project Name: | Project Cont.: COASTAL LAFAYETTE | Project Engr:
Mix Type: Wearing Course | Mix Use: ML - Wearing

Aggregate

Material	Source Code	Aggr. Type	Aggr. %	Bulk Sp Gr, Gsb	Abs.	FAA	Sand Eq	Flat& Elong	CAA	Fr. Rate	%Ret #8
Cr. Aggr	APS00007480	1003M00110-78'S	31.5	2.681	0.6			0.9	100	II	96
Cr. Aggr	APS00007480	1003M00120-8'S	16.1	2.675	0.6	43		1	100	II	98
RAP Aggr	PS00000630	1003M01000-SCR. RAP PD	19.3	2.601							54
Fine Aggr	APS00007480	1003M00110-W11'S	21.0	2.671	0.8	46				II	22
Fine Aggr	APS00007040	1003M00110-T. SAND	12.1	2.631	0.5	38	95				10
Composite			GSB	2.656	0.64	42	95	0.9	100		

Asphalt Cement and Additives

Material	Source Code	Material Name	% of Mix
Asphalt Cement	APS00000400	1002M00040-PG70-22M Marathon	4.3
Alternate Asphalt			
Alternate Asphalt			
Rap Asphalt			0.7
Anti Strip	APS00003920	1002M00220-Anti-Strip	0.7

DESIGN DATA		VALIDATION DATA			JMF Limits (per valid.avg)		
Parameter	Submittal	Average	Std. Dev	PWL			
Gmm	2.471			--		--	
%Gmm,Nini	88.3			--			91
%Gmm,Nmax	97.1			--		--	98
VMA	14.7			--	13.5	--	
VFA	76			--	69	--	80
% Voids	3.5			--	2.5	--	4.5
% Design AC	5.0						
Comp Temp	300			--		--	
% DF Crushed	99				75	--	
1 1/2 (37.5mm)	100			--		--	
1 in (25mm)	100			--		--	
3/4 (19mm)	100			--		--	
1/2in (12.5mm)	97			--		--	
3/8in (9.5mm)	85			--		--	
No. 4 (4.75mm)	52			--		--	
No. 8(2.36mm)	37			--		--	
No.16(1.18mm)	28			--		--	
No.30(600um)	22			--		--	
No.50(300um)	12			--		--	
No100(150um)	6			--		--	
No. 200(75um)	4.6			--		--	
% AC Extracted	5.0			--		--	
Dust/Pbeff	0.96			--	0.6	--	1.6
Gse	2.867						
Pba	0.17				≥ 0.0		
Pbe	4.8						

Remarks: DISCHARGE 300 RANGE 275-325
GRAVITIES UP DATED TO CURRENT GRAVITIES.

Loaded Wheel Test

Design: No. Passes 20000
Rut 2.90

Validation: No. Passes 0
Rut

SCB Jc: 0.64

Submitted for Contractor By: 0971
Date Submitted 03/07/19

Kent Langley
Technician

Proposal Approved Y=Yes N=No: Y
By: 0304
Date 3/7/2019

Signature

Validation Approved Y=Yes N=No
By:
Date

Number of Validation Attempts

(y/n)
LWT = PASS ....
Each PWL Parameter ≥ 71 ....
Avg. within JMF spec. limits ....

Approved By

Date First Used

LaPave 502 v17.05.18

3/7/2019

JMF of Mix 2

Louisiana Department of Transportation and Development
JMF SUPERPAVE ASPHALTIC CONCRETE MIXTURES

Metric/English	E	Plant Code	PS00000630-Coastal Bridge, Inc., LLC - Lafayette	SMM ID	0
Project No.	H.012176.6				
Specs	2016	Plant Type	3-dryer drum	Mix Type	Wearing Course
Mix Use	ML - Wearing	Des.Level	SMA		
ESAL	0	Prod.Rate	350	Mix Temp	325
Seq No	180				
Adj. Factor	1.00	ADT/lane	47900	Nom.Agg.Size	0.5 in.
AC Corr Factor	0.08				
Project Name	I-10	Project Cont.	COASTAL LAFAYETTE	Project Engr	Beau Istre
		Mix Type	Wearing Course	Mix Use	ML - Wearing

Aggregate

Material	Source Code	Aggr. Type	Aggr. %	Bulk Sp Gr, Gsb	Abs.	FAA	Sand Eq	Flat& Elong	CAA	Fr. Rate	%Ret #8
Cr. Aggr	APS00006750	1003M00120-#7 GRAN	35.5	2.663	1.5			1	100	I	96
Cr. Aggr	APS00007480	1003M00120-LS78	45.7	2.681	0.7			1	100	II	99
Fine Aggr	APS00011430	1003M00110-AGG LIME	18.8	2.632	1.4	45				III	3
Composite			GSB	2.665	1.12	45		1.0	100		

Asphalt Cement and Additives

Material	Source Code	Material Name	% of Mix
Asphalt Cement	PS00000630	1002M00250-PG82-22RM	6.0
Alternate Asphalt			
Alternate Asphalt			
Rap Asphalt			0.0
Anti Strip	APS00011510	1002M00220-EZ	0.1200

DESIGN DATA		VALIDATION DATA			JMF Limits (per valid.avg)		
Parameter	Submittal	Average	Std. Dev	PWL			
Gmm	2.459	2.463	0.00442	100	2.439	--	2.487
%Gmm,Nini	86.1	86.3	0.550	100			90
%Gmm,Nmax				100		--	98
VMA	16.3	16.2	0.207	77	16.0	--	
VFA	79	78	2.30	0	69	--	0
% Voids	3.5	3.5	0.374	100	2.5	--	4.5
% Design AC	6.0						
Comp Temp	300	300	0.00	--	275	--	325
% DF Crushed	100	99	1.34		98	--	
1 1/2 (37.5mm)	100	100	0.00	--	96	--	100
1 in (25mm)	100	100	0.00	--	96	--	100
3/4 (19mm)	100	100	0.00	--	96	--	100
1/2in (12.5mm)	94	93	1.58	100	89	--	97
3/8in (9.5mm)	64	70	5.09	54	66	--	74
No. 4 (4.75mm)	25	27	2.65	94	23	--	31
No. 8(2.38mm)	19	19	1.50	100	16	--	22
No.16(1.18mm)	16	17	1.30	94	15	--	19
No.30(600um)	15	15	1.13	100	13	--	17
No.50(300um)	12	14	0.85	100	12	--	16
No100(150um)	9	13	0.84	100	11	--	15
No. 200(75um)	7.2	8.6	0.604	76	7.9	--	9.3
% AC Extracted	6.0	6.0	0.055	100	5.8	--	6.2
Dust/Pbeff	1.31	1.57	0.1007	60	0.6	--	1.6
Gse	2.697	2.703	0.00572				
Pba	0.46	0.54	0.0894		≥ 0.0		
Pbe	5.5	5.5	0.089				

Remarks: discharge temp 325 range 300-350 zydex ez approved @0.05% using 0.12%
Valero PG-67-22 +10% GTR with 1.1% Additive

Loaded Wheel Test

Design:	No. Passes	20000
	Rut	4.48
Validation:	No. Passes	20000
	Rut	6.04

SCB Jc: 0.84

Submitted for Contractor By: 0971
Date Submitted: 03/22/19

Kent Langley
Technician

Proposal Approved (Y=Yes, N=No): Y
By: 0304
Date: 3/29/2019

Signature

Validation Approved (Y=Yes, N=No): Y
By: 0304
Date: 4/30/2019

Number of Validation Attempts: 1

(y/n)
LWT = PASS .... Y
Each PWL Parameter ≥ 71 .... Y
Avg. within JMF spec. limits .... Y

Approved By

Date First Used

LaPave 502 v17.05.18

4/30/2019

JMF of Mix 3

Louisiana Department of Transportation and Development
JMF SUPERPAVE ASPHALTIC CONCRETE MIXTURES

Metric/English	E	Plant Code	PS00000660-Madden Contracting Company - Shreveport			SMM ID	0
Project No.	H.008575						
Specs	2016	Plant Type	3-dryer drum	Mix Type	Binder Course	Mix Use	ML - Binder
Dec.Level	2						
ESAL	0	Prod.Rate	250	Mix Temp	325	Seq No	88
Adj. Factor	1.00	ADT/lane	0	Nom.Agg.Size	0.75 in.	AC Corr Factor	0.15
Project Name	I-20-CADDO PAR.	Project Cont.	MADDEN CONTR.			Project Engr	MICHAEL RISTER
		Mix Type	Binder Course			Mix Use	ML - Binder

Aggregate

Material	Source Code	Aggr. Type	Aggr. %	Bulk Sp Gr, Gsb	Abs.	FAA	Sand Eq	Flat& Elong	CAA	Fr. Rate	%Ret #8
Cr. Aggr	APS00006730	1003M00120-1' STONE-M/M	15.0	2.879	0.7			0	100	II	98
Cr. Aggr	APS00006730	1003M00120-5/8" STONE-M/M	26.0	2.891	0.5			0	100	II	88
Cr. Aggr	APS00006730	1003M00120-1/2" STONE-M/M	16.5	2.881	1.3			0	100	II	90
RAP Aggr	PS00000660	1003M01000-ARAP-MADDEN	23.8	2.820	0.5			0	100	III	50
Fine Aggr	APS00006730	1003M00110-WASH SCREENS-M/M	10.0	2.844	1.1	44				II	23
Fine Aggr	APS00011330	1003M00110-COARSE SAND-BLOUNT BR.	8.7	2.818	0.8	45	75				100
Composite			GSB	2.858	0.73	45	75	0.0	100		

Asphalt Cement and Additives

Material	Source Code	Material Name	% of Mix
Asphalt Cement	APS00000390	1002M00050-LION/TRINITY PG 76-22	3.4
Alternate Asphalt			
Alternate Asphalt			
Rap Asphalt			1.2
Anti Strip	APS00003920	1002M00220-Anti-Strip-AD-HERE LA-2	0.8

Loaded Wheel Test

Design:	No. Passes	20000	
	Rut	3.29	
Validation:	No. Passes	20000	
	Rut	-2.02	
SCB Jc:	0.88		

DESIGN DATA		VALIDATION DATA			JMF Limits		
Parameter	Submittal	Average	Std. Dev	PWL	(per valid.avg)		
Gmm	2.606	2.609	0.00319	100	2.485	–	2.533
%Gmm,Nini	88.8	89.1	0.779	88			90
%Gmm,Nmax	97.5	97.4	0.838	100		–	98
VMA	13.2	13.2	0.179	100	12.5	–	
VFA	73	72	0.84	100	69	–	80
% Voids	3.5	3.7	0.134	100	2.5	–	4.5
% Design AC	4.8						
Comp Temp	0	300	0.00	–	275	–	325
% DF Crushed	100	40	54.77		95	–	
1 1/2 (37.5mm)	100	100	0.00	–	96	–	100
1 in (25mm)	100	100	0.00	–	96	–	100
3/4 (19mm)	98	98	2.30	97	92	–	100
1/2in (12.5mm)	78	79	2.60	98	75	–	83
3/8in (9.5mm)	63	63	3.31	80	59	–	67
No. 4 (4.75mm)	40	41	3.14	82	37	–	45
No. 8(2.38mm)	30	30	2.38	82	27	–	33
No.16(1.18mm)	26	24	1.88	80	22	–	26
No.30(600um)	18	20	1.22	88	18	–	22
No.50(300um)	12	15	0.89	100	13	–	17
No100(150um)	7	8	0.47	100	6	–	10
No. 200(75um)	4.2	4.4	0.367	100	3.7	–	5.1
% AC Extracted	4.8	4.6	0.098	100	4.4	–	4.8
Dust/Pbeff	1.02	1.09	0.1022	100	0.6	–	1.6
Gse	2.881	2.898	0.00370				
Pba	0.50	0.58	0.0648		≥ 0.0		
Pbe	4.1	4.0	0.055				

Remarks: LEV 2 BINDER

Submitted for Contractor By:

Date Submitted 11/01/17

STEVE MILAM

Technician

Proposal Approved Y=Yes N=No Y

By:

Date

Signature

Validation Approved Y=Yes N=No Y

By:

Date

Number of Validation Attempts		1
		(y/n)
LWT = PASS	....	P
Each PWL Parameter ≥ 71	....	Y
Avg. within JMF spec. limits	....	Y

Approved By

Date First Used 1/14/2018

JMF of Mix 4

Louisiana Department of Transportation and Development
JMF SUPERPAVE ASPHALTIC CONCRETE MIXTURES

Metric/English	E	Plant Code	PS00000660-Madden Contracting Company - Shreveport	SMM ID	0
Project No.	H.009576				
Specs	2016	Plant Type	3-dryer drum	Mix Type	Wearing Course
Mix Use	ML - Wearing	Dec.Level	SMA		
ESAL	0	Prod.Rate	250	Mix Temp	325
Seq No	89				
Adj. Factor	1.00	ADT/lane	0	Nom.Agg.Size	0.5 in.
AC Corr Factor	0.65				
Project Name	I-20-CADDO PAR.	Project Cont.	MADDEN CONTR.	Project Engr	MICHAEL RISTER
		Mix Type	Wearing Course	Mix Use	ML - Wearing

Aggregate

Material	Source Code	Aggr. Type	Aggr. %	Bulk Sp Gr, Gsb	Abs.	FAA	Sand Eq	Flat& Elong	CAA	Fr. Rate	%Ret #8
Cr. Aggr	APS00006730	1003M00120-5/8" STONE-M/M	20.0	2.691	0.5						98
Cr. Aggr	APS00006730	1003M00120-1/2" STONE-M/M	25.0	2.661	1.3			0	100	II	90
Cr. Aggr	APS00006730	1003M00120-1/2" STONE ARK.CLASS 1-M/M	35.0	2.641	1.3			0	100	II	88
Fine Aggr	APS00006120	1003M00110-DONNAFILL-3M	19.9	2.587	0.8	48		0	100	II	0
	1002MO230	CELL. FIBER-HI-TECH ASPH.SOLUTIONS	0.1								
			0.0								
Composite			GSB	2.647	1.04	48		0.0	100		

Asphalt Cement and Additives

Material	Source Code	Material Name	% of Mix
Asphalt Cement	APS00000380	1002M00050-LION/TRINITY PG 76-22	6.3
Alternate Asphalt			
Alternate Asphalt			
Rap Asphalt			0.0
Anti Strip	APS00003920	1002M00220-Anti-Strip-AD-HERE LA-2	0.6

Loaded Wheel Test

Design:	No. Passes	20000
	Rut	5.00
Validation:	No. Passes	20000
	Rut	-4.86
SCB Jc:	0.6	

DESIGN DATA		VALIDATION DATA			JMF Limits (per valid.avg)		
Parameter	Submittal	Average	Std. Dev	PWL			
Gmm	2.430	2.448	0.00573	100	2.424	–	2.472
%Gmm,Nini	88.8	87.0	0.623	100			90
%Gmm,Nmax	97.4	96.8	0.937	94		–	98
VMA	17.0	16.7	0.613	82	16.0	–	
VFA	79	77	2.17	0	69	–	0
% Voids	3.5	3.9	0.458	94	2.5	–	4.5
% Design AC	6.3						
Comp Temp	300	300	0.00	–	275	–	325
% DF Crushed	100	100	0.00		98	–	
1 1/2 (37.5mm)	100	100	0.00	–	96	–	100
1 in (25mm)	100	100	0.00	–	96	–	100
3/4 (19mm)	100	100	0.00	–	96	–	100
1/2in (12.5mm)	92	92	1.71	100	88	–	96
3/8in (9.5mm)	73	76	1.88	100	72	–	80
No. 4 (4.75mm)	30	32	1.28	100	28	–	36
No. 8(2.36mm)	23	22	1.49	100	19	–	25
No.16(1.18mm)	21	20	1.42	80	18	–	22
No.30(600um)	20	20	1.41	80	18	–	22
No.50(300um)	17	15	1.08	100	13	–	17
No100(150um)	11	11	0.78	100	9	–	13
No. 200(75um)	7.8	7.1	0.555	82	6.4	–	7.8
% AC Extracted	6.3	6.2	0.084	100	6.0	–	6.4
Dust/Pbeff	1.29	1.28	0.1007	100	0.6	–	1.6
Gse	2.674	2.698	0.00719				
Pba	0.40	0.72	0.1095		≥ 0.0		
Pbe	5.9	5.6	0.071				

Submitted for Contractor By:	201
Date Submitted	11/01/17

STEVE MILAM

Technician

Proposal Approved	Y=Yes	
	N=No	
By:		
Date		

Signature

Validation Approved	Y=Yes	Y
	N=No	
By:		
Date		
Number of Validation Attempts		1
		(y/n)
LWT = PASS	....	Y
Each PWL Parameter	≥ 71	Y
Avg. within JMF spec. limits	....	Y

Approved By

Date First Used

Remarks: SMA-3 H-425

LaPave 502 v17.05.18 7/12/2023

JMF of Mix 5

Lousiana Department of Transportation and Development
JMF SUPERPAVE ASPHALTIC CONCRETE MIXTURES

Mix ID	00650-0003v1	Custom Name	JMF 320				
Des.Level	1	Plant Code	PS00000650 - Madden Contracting Company - Sibley				
Mix Type	Wearing Course	Mix Temp	325	AC Corr Factor	-0.28	ADT	1000 - 3500
Nom.Agg.Size	1/2 in.	Prod.Rate	250	Adj.Factor	1.00	Specs	2018

	Supplier Code	Material Code	Custom Name	Agg %	Appr. Gravity	Bulk Grav.	Absp	FAA	Sand Eq	Flat Elng	CAA	Frictn Rate	Ret #4	Ret #8
C	APS00006710	1003M00120	Cove 1/2"	34.0	2.712	2.647	0.9			0.0	100	II	87	96
C	APS00006710	1003M00120	Cove 5/8"	10.0	2.705	2.662	0.6			0.0	100	II	91	94
C	APS00006710	1003M00120	Cove Scree	10.0	2.727	2.641	1.2	47				II	7	38
C	APS00006710	1003M00120	Wash Scree	16.0	2.717	2.652	0.9	49				II	17	49
F	APS00012660	1003M00110	Coarse Sar	10.9	2.678	2.636	0.6	42	75				2	3
R	PS00000650	1003M01000	Minden Fra	19.1	2.628	2.594	0.5				100		32	49
	Combined Aggregate Properties			100	2.694	2.637	0.8	45	75	0	100			

P/S	Material Code	Name	% Mix	Pass/Max Rut	LWT(des)	LWT(val)	SCB
APS00000360	1002M00035	Ergon 67-22	4.1	20000/10	5.69		0.61
APS00000390	1002M00035	Lion Oil 67-22	---				
APS00010870	1002M00035	Martin 67-22	---				
APS00011510	1002M00220	ZycoTherm SP	0.06				
		Total %AC from RAP	0.9				

DESIGN		VALIDATION			
Parameter	Submittal	Average	Std.Dev.	PWL	JMF Limits
Gmm	2.466	2.481			2.466 - 2.496
%Gmm,Ni	88.6	89.2			Max 91.0
%Gmm,Nm	97.9				Max 98.0
Gmb,Nd	2.385	2.389			2.365 - 2.413
VMA	14.1	13.8			Min 13.5
VFA	77	74			69 - 80
%Voids	3.3	3.7			2.5 - 4.5
% AC	5	5			
Gse	2.661	2.679			
Pba	0.35	0.7			
Pbe	4.7	4.3			
Dust/Pbeff	1.17	1.25			
Crushed	100	100			
Pass 1 1/2"	100	100			96 - 100
Pass 1"	100	100			96 - 100
Pass 3/4"	100	100			96 - 100
Pass 1/2"	93	94			90 - 98
Pass 3/8"	81	83			79 - 87
Pass No.4	50	50			46 - 54
Pass No.8	38	36			33 - 39
Pass No.16	31	28			26 - 30
Pass No.30	26	24			22 - 26
Pass No.50	18	18			16 - 20
Pass No.100	10	10			8 - 12
Pass No.200	5.5	5.4			4.7 - 6.1

Submitted to District 04

Campbell, Taylor cmdc0010
Submitted By

8/12/2019
Date Submitted

Bryant, Rachel d04x4
Checked By

8/12/2019
Date Checked

Allen, Jeffery d04k4
Approved By

8/12/2019
Date Approved

d04k4 Allen, Jeffery
Conditionally Validated By

8/12/2019
Date Validated

d04k4 Allen, Jeffery
Validation Approval By

8/12/2019
Date Final Approved Validation

JMF of Mix 6

Louisiana Department of Transportation and Development
JMF SUPERPAVE ASPHALTIC CONCRETE MIXTURES

Metric/English	E	Plant Code	PS00000630-Coastal Bridge, Inc., LLC - Lafayette	SMM ID	0
Project No.	H010248				
Specs	2016	Plant Type	3-dryer drum	Mix Type	Wearing Course
Mix Use	ML - Wearing	Des.Level	2F		
ESAL	4,002,826	Prod.Rate	350	Mix Temp	300
Seq No	158				
Adj. Factor	1.00	ADT/lane	15800	Nom.Agg.Size	0.5 in.
AC Corr Factor	0.08				
Project Name	LA28	Project Cont.	COASTAL LAF.	Project Engr	BEAU ISTRE
		Mix Type	Wearing Course	Mix Use	ML - Wearing

Aggregate

Material	Source Code	Aggr. Type	Aggr. %	Bulk Sp Gr, Gsb	Abs.	FAA	Sand Eq	Flat& Elong	CAA	Fr. Rate	%Ret #8
Cr. Aggr	APS00006370	1003M00120-SANDSTONE	30.0	2.631	0.9	42		1	100	I	91
Cr. Aggr	APS00007480	1003M00120-78'S	13.0	2.890	0.6			0.9	100	II	97
Cr. Aggr	APS00007480	1003M00120-8'S	13.5	2.891	0.6	43		1	100	II	96
RAP Aggr	PS00000630	1003M01000-SCR RAP LAF	19.2	2.540							48
Fine Aggr	APS00007480	1003M00110-W11'S	16.1	2.671	0.8	46				II	33
Fine Aggr	APS00012000	1003M00110-P. SAND	8.2	2.635	0.3	43	89				0
Composite			GSB	2.635	0.72	45	89	1.0	100		

Asphalt Cement and Additives

Material	Source Code	Material Name	% of Mix
Asphalt Cement	PS00000400	1002M00050-76-22M	4.2
Alternate Asphalt			
Alternate Asphalt			
Rap Asphalt			0.8
Anti Strip	APS00003920	1002M00220-Anti-Strip	0.7

DESIGN DATA		VALIDATION DATA			JMF Limits		
Parameter	Submittal	Average	Std. Dev	PWL	(per valid.avg)		
Gmm	2.448	2.494	0.00110	100	2.470	–	2.518
%Gmm,Nini	88.5	88.2	1.188	97			90
%Gmm,Nmax	97.7	97.7	0.192	91		–	98
VMA	14.8	13.5	0.422	64	13.5	–	
VFA	76	72	2.69	88	69	–	80
% Voids	3.5	3.8	0.518	91	2.5	–	4.5
% Design AC	5.0						
Comp Temp	300	300	0.00	–	275	–	325
% DF Crushed	89				95	–	
1 1/2 (37.5mm)	100	100	0.00	–	96	–	100
1 in (25mm)	100	100	0.00	–	96	–	100
3/4 (19mm)	100	100	0.00	–	96	–	100
1/2in (12.5mm)	94	95	0.54	100	91	–	99
3/8in (9.5mm)	80	82	0.83	100	78	–	86
No. 4 (4.75mm)	45	45	0.80	100	41	–	49
No. 8(2.36mm)	35	32	0.81	100	29	–	35
No.16(1.18mm)	28	26	0.69	100	24	–	28
No.30(600um)	22	23	0.84	100	21	–	25
No.50(300um)	12	16	0.47	100	14	–	18
No100(150um)	7	9	0.82	100	7	–	11
No. 200(75um)	4.9	6.0	0.554	82	5.3	–	6.7
% AC Extracted	5.0	4.7	0.055	100	4.5	–	4.9
Dust/Pbeff	0.88	1.48	0.1358	86	0.6	–	1.6
Gse	2.839	2.898	0.00141				
Pba	0.06	0.90	0.0000		≥ 0.0		
Pbe	5.0	4.1	0.000				

Loaded Wheel Test

Design: No. Passes 20000; Rut 4.71

Validation: No. Passes 0; Rut

SCB Jc: 0.78

Submitted for Contractor By: 971

Date Submitted 02/02/18

Ryan Maddox

Technician

Proposal Approved Y=Yes N=No Y

By: 304

Date 6/1/2018

Signature

Validation Approved Y=Yes N=No

By:

Date

Number of Validation Attempts

(y/n)

LWT = PASS . . . .

Each PWL Parameter ≥ 71 . . . .

Avg. within JMF spec. limits . . . .

Approved By

Date First Used

Remarks: DISCHARGE TEMP 300 RANGE 275-325

Special Provisions 01/17

JMF of Mix 7

LOUISIANA SUPERPAVE JMF RELEASE FORM(05/18/98)

Project No.		Plant Code		Mix Code	26	Date of Spec.	2018
Proj. Eng.		JMF Seq. No.				For Batch Plants	
Des.Level	1	Mix Type	Wearing	Nom.Max.Agg. Size	12.5	Dry Mix Time	
Traffic(ADT)		Plant Type	Double Barre	Use	Wearing	Wet Mix Time	
Sub. By Cont.	Prairie Contractors	Prod.Rate (Mg/hr.)	350				

Source Code	Source	Aggregate Type	%	Apparent Gravity	Bulk Gravity	% Abs.	FAA Meth."A"	Sand Equiv. -4.75mm	Flat&Elong % 5:1	CAA +2Faces	Frict. Rating
				1.000	1.000						
ABBQ	Vulcan	#78LS	20.8	2.712	2.683	0.40			0.10	100.0	3
				1.000	1.000						
				1.000	1.000						
				1.000	1.000						
ABBQ	Vulcan	#89 LS	17.7	2.699	2.670	0.40					
ABBQ	Vulcan	#11LS	34.3	2.700	2.671	0.40	49.00	69.00		100.0	3
	Durrand	CoarseSand	12.9	2.655	2.627	0.40	41.00	93.00			
				1.000	1.000						
				1.000	1.000						
Prairie	Diamond-B	Rap	14.3	2.591	2.591						
ıbined Agg. Properties			100.0	2.680	2.656						

Mix Gravities 2.494 2.474 **'Total Asphalt%** 4.7

	Code	Material Name		Source		%	Sp.Grav.
Virgin Asphalt		PG-67-22		Martin		4.0	1.030
Rec.AC Credit	Prairie	Rap		Prairie		0.7	2.591
Anti-Strip	5730	ADHERELA2		ARR MAZ		0.6	

Design Submitted by Contractor

Average Volumetrics

Gmm	2.484
%Gmm,Ni	89.7
%Gmm,Nd	96.6
%Gmm,Nmax	96.6
Gmb@des.est.	2.399
Gmb@des.cor.	2.399
VMA	13.9
VFA	76
%Voids	3.4
%Desn.AC	4.7
Gsb Agg.	2.656
Slope	7.73
Comp.Temp.	300
Gmb(Max)	2.399
%Crushed	100.0

Average Oven Extracted

Sieve	%Passing
1 1/2"	100
1"	100
3/4"	100
1/2"	97
3/8"	88
#4	63
#8	44
#16	33
#30	26
#50	16
#100	8
#200	5.5
%Extr.AC	5.0
Dust/Peff.	1.21
Pa Abs.	0.160
Pbe	4.50
Gse Est.	2.675
Gb	1.030
Gse	2.668

AVG.GYRATORY DATA AT OPTIMUM AC

'%Design AC 4.7 **GSB** 2.656

Specimen No. 1

Gmm 2.484

	Gyration	Ht,mm	Gmb(est)	Gmb(corr)	%Gmm
N Initial	7	123.3	2.229	2.229	89.8
N Design	55	114.5	2.400	2.400	96.7
N Max	55	114.5	2.400	2.400	96.7
	Gmb	2.400	Corr. Factor		1.000

Air Wt.	Water Wt.	SSD Wt.
4751.5	2785.4	4764.8

VMA	13.8
VFA	76
Voids	3.3
Slope	7.71

Specimen No. 2

Gmm 2.484

	Gyration	Ht,mm	Gmb(est)	Gmb(corr)	%Gmm
N Initial	7	123.7	2.225	2.225	89.6
N Design	55	114.8	2.398	2.398	96.6
N Max	90	114.8	2.398	2.398	96.6
	Gmb	2.398	Corr. Factor		1.000

Air Wt.	Water Wt.	SSD Wt.
4748.3	2783.7	4763.9

VMA	13.9
VFA	75
Voids	3.4
Slope	7.76

AASHTO T283 as Modified by PP28

Control PSI

TSR % #DIV/0!

Opt.Mixing Temp. 325

Opt. Comp. Temp. 300

Submitted for Contractor by: Barry L. Nunez

Date Submitted:

Proposal Approved by: **Validation Approved by:**

Date Approved: **Date Approved:**

Remarks:

JMF of Mix 8

β.00

LOUISIANA SUPERPAVE JMF RELEASE FORM(05/18/98)

Project No.		Plant Code		Mix Code	26	Date of Spec.	2018
Proj. Eng.		JMF Seq. No.				For Batch Plants	
Des.Level	1	Mix Type	Wearing	Nom.Max.Agg. Size	12.5	Dry Mix Time	
Traffic(ADT)		Plant Type	Double Barre	Use	Wearing	Wet Mix Time	
Sub. By Cont.	Prairie Contractors	Prod.Rate (Mg/hr.)	350				

Source Code	Source	Aggregate Type	%	Apparent Gravity	Bulk Gravity	% Abs.	FAA Meth."A"	Sand Equiv. -4.75mm	Flat&Elong % 5:1	CAA +2Faces	Frict. Rating
				1.000	1.000						
ABBQ	Vulcan	#78LS	20.8	2.712	2.683	0.40			0.10	100.0	3
				1.000	1.000						
				1.000	1.000						
				1.000	1.000						
ABBQ	Vulcan	#89 LS	17.7	2.699	2.670	0.40					
ABBQ	Vulcan	#11LS	34.3	2.700	2.671	0.40	49.00	69.00		100.0	3
	Durrand	CoarseSand	12.9	2.655	2.627	0.40	41.00	93.00			
				1.000	1.000						
				1.000	1.000						
Prairie	Diamond-B	Rap	14.3	2.591	2.591						
mbined Agg. Properties			100.0	2.680	2.656						

Mix Gravities 2.494 2.474 **'Total Asphalt%** 4.7

	Code	Material Name		Source		%	Sp.Grav.
Virgin Asphalt		PG-67-22		Martin		4.0	1.030
Rec.AC Credit	Prairie	Rap		Prairie		0.7	2.591
Anti-Strip	5730	ADHERELA2		ARR MAZ		0.6	

Design Submitted by Contractor

Average Volumetrics

Gmm	**2.484**
%Gmm,Ni	89.7
%Gmm,Nd	96.6
%Gmm,Nmax	96.6
Gmb@des.est	2.399
Gmb@des.cor	2.399
VMA	13.9
VFA	76
%Voids	3.4
%Desn.AC	4.7
Gsb Agg.	2.656
Slope	7.73
Comp.Temp.	300
Gmb(Max)	2.399
%Crushed	100.0

Average Oven Extracted

Sieve	%Passing
1 1/2"	100
1"	100
3/4"	100
1/2"	97
3/8"	88
#4	63
#8	44
#16	33
#30	26
#50	16
#100	8
#200	5.5
%Extr.AC	5.0
Dust/Peff.	1.21
Pa Abs.	0.160
Pbe	4.50
Gse Est.	2.675
Gb	1.030
Gse	2.668

AVG.GYRATORY DATA AT OPTIMUM AC

'%Design AC 4.7 **GSB** 2.656

Gmm 2.484 **Specimen No. 1**

	Gyration	Ht,mm	Gmb(est)	Gmb(corr)	%Gmm
N Initial	7	123.3	2.229	2.229	89.8
N Design	55	114.5	2.400	2.400	96.7
N Max	55	114.5	2.400	2.400	96.7
	Gmb	2.400	Corr. Factor		1.000

Air Wt.	Water Wt.	SSD Wt.
4751.5	2785.4	4764.8
VMA	13.8	
VFA	76	
Voids	3.3	
Slope	7.71	

Gmm 2.484 **Specimen No. 2**

	Gyration	Ht,mm	Gmb(est)	Gmb(corr)	%Gmm
N Initial	7	123.7	2.225	2.225	89.6
N Design	55	114.8	2.398	2.398	96.6
N Max	90	114.8	2.398	2.398	96.6
	Gmb	2.398	Corr. Factor		1.000

Air Wt.	Water Wt.	SSD Wt.
4748.3	2783.7	4763.9
VMA	13.9	
VFA	75	
Voids	3.4	
Slope	7.76	

AASHTO T283 as Modified by PP28

Control PSI

TSR % #DIV/0!

Opt.Mixing Temp. 325

Opt. Comp. Temp. 300

Submitted for Contractor by: Barry L. Nunez

Date Submitted:

Proposal Approved by: **Validation Approved by:**

Date Approved: **Date Approved:**

Remarks:

JMF of Mix 9

Lousiana Department of Transportation and Development

JMF SUPERPAVE ASPHALTIC CONCRETE MIXTURES

Mix ID	00810-0001v4	Custom Name	JMF 08				
Des.Level	1	Plant Code	PS00000810 - Madden Construction Company #AP16 - Campti				
Mix Type	Binder Course	Mix Temp	325	AC Corr Factor	-0.1	ADT	1000 - 3500
Nom.Agg.Size	3/4 in.	Prod.Rate	250	Adj.Factor	1.00	Specs	2018

	Supplier Code	Material Code	Custom Name	Agg %	Appr. Gravity	Bulk Grav.	Absp	FAA	Sand Eq	Flat Elng	CAA	Frictn Rate	Ret #4	Ret #8
C	APS00006710	1003M00120	Cove 1/2"	24.0	2.700	2.643	0.8			0.0	100	II	87	96
C	APS00006710	1003M00120	Cove 5/8"	24.2	2.702	2.659	0.6			0.0	100	II	91	94
F	APS00006710	1003M00110	Cove Dirty S	8.0	2.674	2.604	1.0	48					7	38
F	APS00006710	1003M00110	Cove Wash	10.0	2.704	2.640	0.9	49					17	49
F	APS00012660	1003M04300	Skyplex Sa	10.1	2.648	2.620	0.4	40	78				0	2
R	PS00000810	1003M01000	Natchitoche	23.7	2.679	2.609	1.0				86		30	48
Combined Aggregate Properties				100	2.689	2.633	0.8	44	78	0	95			

P/S	Material Code	Name	% Mix	Pass/Max Rut	LWT(des)	LWT(val)	SCB
APS00000360	1002M00035	Ergon 67-22	3.3	20000/10	3.2	4.3	0.54
APS00000390	1002M00035	Delek 67-22	—	20000/10	3.28	4.8	0.79
APS00010870	1002M00035	Martin 67-22	—				
APS00003920	1002M00220	LA-2 Anti-strip	0.60				
		Total %AC from RAP	1.3				

DESIGN		VALIDATION			
Parameter	Submittal	Average	Std.Dev.	PWL	JMF Limits
Gmm	2.488	2.48	0.003271	100	2.465 - 2.495
%Gmm,Ni	87.9	89.8	0.24495	100	Max 91.0
%Gmm,Nm	97.4	97.8			Max 98.0
Gmb,Nd	2.398	2.401	0.0066332		2.377 - 2.425
VMA	13.1	12.9	0.22804		Min 12.5
VFA	72	75	1.3416	100	69 - 80
%Voids	3.6	3.2	0.24495	100	2.5 - 4.5
% AC	4.6	4.7	0.08367		
Gse	2.67	2.661	0.0072664		
Pba	0.54	0.5	0.10512		
Pbe	4.1	4.1	0.05477		
Dust/Pbeff	1.2	1.13	0.060992		
Crushed	100	100	0	100	
Pass 1 1/2"	100	100	0	100	96 - 100
Pass 1"	100	100	0	100	96 - 100
Pass 3/4"	100	100	0	100	96 - 100
Pass 1/2"	83	86	1.4832		82 - 90
Pass 3/8"	73	73	2		69 - 77
Pass No.4	49	45	1.9235		41 - 49
Pass No.8	34	34	1.4142	100	31 - 37
Pass No.16	28	27	0.8944		25 - 29
Pass No.30	22	22	0.5477		20 - 24
Pass No.50	14	13	0.5477		11 - 15
Pass No.100	8	7	0.4472		5 - 9
Pass No.200	4.9	4.7	0.23452	100	4 - 5.4

Submitted to District 08

Campbell, Taylor cmdc0010
Submitted By

10/30/2019
Date Submitted

James, Chris 00273003
Checked By

10/30/2019
Date Checked

James, Chris 00273003
Approved By

10/30/2019
Date Approved

00273003 James, Chris
Conditionally Validated By

11/8/2019
Date Validated

00273003 James, Chris
Validation Approval By

11/8/2019
Date Final Approved Validation

JMF of Mix 10

Lousiana Department of Transportation and Development

JMF SUPERPAVE ASPHALTIC CONCRETE MIXTURES

Mix ID	00810-0002v3	Custom Name	JMF 13				
Des.Level	1	Plant Code	PS00000810 - Madden Construction Company #AP16 - Campti				
Mix Type	Wearing Course	Mix Temp	325	AC Corr Factor	-0.28	ADT	1000 - 3500
Nom.Agg.Size	1/2 in.	Prod.Rate	250	Adj.Factor	1.00	Specs	2018

	Supplier Code	Material Code	Custom Name	Agg %	Appr. Gravity	Bulk Grav.	Absp	FAA	Sand Eq	Flat Elng	CAA	Frictn Rate	Ret #4	Ret #8
C	APS00006710	1003M00120	Cove 1/2"	34.0	2.700	2.643	0.8			0.0	100	II	87	96
C	APS00006710	1003M00120	Cove 5/8"	10.0	2.702	2.659	0.6			0.0	100	II	91	94
F	APS00006710	1003M00110	Cove Dirty :	10.0	2.674	2.604	1.0	48					7	38
F	APS00006710	1003M00110	Cove Wash	16.0	2.704	2.640	0.9	49					17	49
F	APS00012660	1003M04300	Skyplex Sa	11.0	2.648	2.620	0.4	40	78				0	2
R	PS00000810	1003M01000	Natchitoche	19.0	2.679	2.609	1.0				86		30	48
Combined Aggregate Properties				100	2.689	2.631	0.8	45	78	0	96			

P/S	Material Code	Name	% Mix	Pass/Max Rut	LWT(des)	LWT(val)	SCB
APS00000360	1002M00035	Ergon 67-22	4	20000/10	2.88	3.14	0.61
APS00000390	1002M00035	Delek 67-22	---	20000/10	3.04	3.9	
APS00010870	1002M00035	Martin 67-22	---				
APS00003920	1002M00220	LA-2 Anti-strip	0.60				
		Total %AC from RAP	1.0				

DESIGN		VALIDATION			
Parameter	Submittal	Average	Std.Dev.	PWL	JMF Limits
Gmm	2.473	2.479	0.0053198	100	2.464 - 2.494
%Gmm,Ni	88.4	88.9	0.27019	100	Max 91.0
%Gmm,Nm	97.9				Max 98.0
Gmb,Nd	2.385	2.387	0.0041593		2.363 - 2.411
VMA	13.9	13.9	0.16733		Min 13.5
VFA	74	73	1.5166	100	69 - 80
%Voids	3.6	3.7	0.21679	100	2.5 - 4.5
% AC	5	5.1	0.08944		
Gse	2.67	2.679	0.0037815		
Pba	0.57	0.7	0.05454		
Pbe	4.5	4.4	0.14832		
Dust/Pbeff	1.22	1.1	0.021909		
Crushed	100	100	0	100	
Pass 1 1/2"	100	100	0	100	96 - 100
Pass 1"	100	100	0	100	96 - 100
Pass 3/4"	100	100	0	100	96 - 100
Pass 1/2"	93	93	1.1402		89 - 97
Pass 3/8"	81	82	2.7928		78 - 86
Pass No.4	50	49	1.1402		45 - 53
Pass No.8	38	36	0.8944	100	33 - 39
Pass No.16	31	28	0.7071		26 - 30
Pass No.30	26	22	0.4472		20 - 24
Pass No.50	18	14	0	100	12 - 16
Pass No.100	10	7	0.4472		5 - 9
Pass No.200	5.5	4.8	0.11402	100	4.1 - 5.5

Submitted to District 08

Campbell, Taylor cmdc0010
Submitted By

11/1/2019
Date Submitted

James, Chris 00273003
Checked By

11/2/2019
Date Checked

James, Chris 00273003
Approved By

11/2/2019
Date Approved

00273003 James, Chris
Conditionally Validated By

11/6/2019
Date Validated

00273003 James, Chris
Validation Approval By

11/6/2019
Date Final Approved Validation

JMF of Mix 11

Lousiana Department of Transportation and Development

JMF SUPERPAVE ASPHALTIC CONCRETE MIXTURES

ProjectID	H.007873.6	BAYOU BOEUF AND TURNER CANAL BRIDGI		Proj.Eng.	Montalvo, Joseph		
Mix ID	00780-0003v2	Custom Name	JMF11 L1WCR				
Des.Level	1	Plant Code	PS00000780 - Diamond B Construction Company, LLC - Alexandria				
Mix Type	Wearing Course	Mix Temp	325	AC Corr Factor	-0.28	ADT	> 7000
Nom.Agg.Size	1/2 in.	Prod.Rate	250	Adj.Factor	1.00	Specs	2018

	Supplier Code	Material Code	Custom Name	Agg %	Appr. Gravity	Bulk Grav.	Absp	FAA	Sand Eq	Flat Elng	CAA	Frictn Rate	Ret #4	Ret #8
C	APS00007380	1003M00120	#78 Limestc	22.7	2.707	2.678	0.4			0.1	100	II	90	96
C	APS00007380	1003M00120	#89 Limestc	25.1	2.697	2.675	0.3			0.1	100	II	66	90
F	APS00007380	1003M00110	#11 Limestc	21.0	2.700	2.671	0.4	49	93			II	11	35
F	APS00011720	1003M00110	Coarse Sar	12.2	2.662	2.620	0.6	40	70				0	3
R	PS00000780	1003M01000	RAP	19.0	2.628	2.594	1.0						34	51
Combined Aggregate Properties				100	2.683	2.653	0.5	44	85	0.1	100			

P/S	Material Code	Name	% Mix	Pass/Max Rut	LWT(des)	LWT(val)	SCB
PS00000780	1002M00250	PG 67-22+Latex	3.7	20000/10	3.12	4.7	0.92
PS00004710	1002M00300	Latex	2.50				
APS00014940	1002M00220	Anti-Strip	0.60				
		Total %AC from RAP	1.0				

DESIGN		VALIDATION			
Parameter	Submittal	Average	Std.Dev.	PWL	JMF Limits
Gmm	2.476	2.481	0.0083964	100	2.466 - 2.496
%Gmm,Ni	88.7	88.6	0.55045	100	Max 91.0
%Gmm,Nm	97.7	96.8			Max 98.0
Gmb,Nd	2.39	2.379	0.0061807		2.355 - 2.403
VMA	14.1	14.5	0.26833		Min 13.5
VFA	75	72	2.8636	84	69 - 80
%Voids	3.5	4.1	0.43012	82	2.5 - 4.5
% AC	4.7	4.8	0.15166		
Gse	2.66	2.666	0.0043932		
Pba	0.1	0.2	0.06557		
Pbe	4.6	4.5	0.18708		
Dust/Pbeff	1.17	1.27	0.11811		
Crushed	98	100	0	100	
Pass 1 1/2"	100	100	0	100	96 - 100
Pass 1"	100	100	0	100	96 - 100
Pass 3/4"	100	100	0	100	96 - 100
Pass 1/2"	98	97	0.4472		93 - 100
Pass 3/8"	86	89	0.4472		85 - 93
Pass No.4	54	59	1.1402		55 - 63
Pass No.8	38	38	0.5477	100	35 - 41
Pass No.16	30	28	0	100	26 - 30
Pass No.30	22	22	0	100	20 - 24
Pass No.50	12	13	0.5477		11 - 15
Pass No.100	8	8	0.5477		6 - 10
Pass No.200	5.4	5.7	0.34641	100	5 - 6.4

Submitted to District 08

Garza, Tony cdbc0066
Submitted By

8/26/2019
Date Submitted

James, Chris 00273003
Checked By

9/3/2019
Date Checked

James, Chris 00273003
Approved By

9/3/2019
Date Approved

00273003 James, Chris
Conditionally Validated By

9/3/2019
Date Validated

00273003 James, Chris
Validation Approval By

9/3/2019
Date Final Approved Validation

JMF of Mix 12

Lousiana Department of Transportation and Development

JMF SUPERPAVE ASPHALTIC CONCRETE MIXTURES

Mix ID	00810-0007v1	Custom Name	JMF 17				
Des.Level	1F	Plant Code	PS00000810 - Madden Construction Company #AP16 - Campti				
Mix Type	Wearing Course	Mix Temp	325	AC Corr Factor	-0.16	ADT	3500 – 7000
Nom.Agg.Size	1/2 in.	Prod.Rate	250	Adj.Factor	1.00	Specs	2018

	Supplier Code	Material Code	Custom Name	Agg %	Appr. Gravity	Bulk Grav.	Absp	FAA	Sand Eq	Flat Elng	CAA	Frictn Rate	Ret #4	Ret #8
C	APS00006710	1003M00120	Cove 1/2"	34.0	2.700	2.643	0.8			0.0	100	II	87	96
C	APS00006710	1003M00120	Cove 5/8"	10.0	2.702	2.659	0.6			0.0	100	II	91	94
F	APS00006710	1003M00110	Cove Dirty $	10.0	2.674	2.604	1.0	48					7	38
F	APS00006710	1003M00110	Cove Wash	16.0	2.704	2.640	0.9	49					17	49
F	APS00012660	1003M04300	Skyplex Sa	11.0	2.648	2.620	0.4	40	78				0	2
R	PS00000810	1003M01000	Natchitoche	19.0	2.679	2.609	1.0				86		30	48
	Combined Aggregate Properties			100	2.689	2.631	0.8	45	78	0	96			

P/S	Material Code	Name	% Mix	Pass/Max Rut	LWT(des)	LWT(val)	SCB
APS00000360	1002M00040	Ergon 70-22	4.1				
APS00000390	1002M00040	Lion Oil 70-22	—	20000/10	3.96	4.0	0.78
APS00014940	1002M00220	LA-2 Anti-strip	0.60				
		Total %AC from RAP	1.0				

	DESIGN	VALIDATION			
Parameter	Submittal	Average	Std.Dev.	PWL	JMF Limits
Gmm	2.476	2.481	0.0030496	100	2.466 - 2.496
%Gmm,Ni	89	89.1	0.30332	100	Max 91.0
%Gmm,Nm	97.6	97.6			Max 98.0
Gmb,Nd	2.39	2.394	0.0028635		2.37 - 2.418
VMA	13.8	13.6	0.13038		Min 13.5
VFA	75	74	1.6733	100	69 - 80
%Voids	3.5	3.5	0.23875	100	2.5 - 4.5
% AC	5.1	5.1	0.16733		
Gse	2.678	2.682	0.0066708		
Pba	0.69	0.7	0.0946		
Pbe	4.4	4.4	0.11402		
Dust/Pbeff	1.18	1.35	0.04219		
Crushed	100	100	0	100	
Pass 1 1/2"	100	100	0	100	96 - 100
Pass 1"	100	100	0	100	96 - 100
Pass 3/4"	100	100	0	100	96 - 100
Pass 1/2"	94	92	0.8367		88 - 96
Pass 3/8"	83	82	1.6733		78 - 86
Pass No.4	49	51	2.1213		47 - 55
Pass No.8	36	37	1.2247	100	34 - 40
Pass No.16	28	29	1.0954		27 - 31
Pass No.30	23	24	0.8944		22 - 26
Pass No.50	14	15	0.4472		13 - 17
Pass No.100	8	8	0.5477		6 - 10
Pass No.200	5.2	5.9	0.24083	100	5.2 - 6.6

Submitted to District 08

Campbell, Taylor cmdc0010
Submitted By

6/17/2021
Date Submitted

Credeur, David 00323747
Checked By

6/17/2021
Date Checked

Kelly, Jordan d086g
Approved By

6/17/2021
Date Approved

d086g Kelly, Jordan
Conditionally Validated By

8/9/2021
Date Validated

d086g Kelly, Jordan
Validation Approval By

8/9/2021
Date Final Approved Validation

LaPave Online - JMF Report Report By Campbell, Taylor cmdc0010 9/30/2021 8:24:58 AM

JMF of Mix 13

Lousiana Department of Transportation and Development
JMF SUPERPAVE ASPHALTIC CONCRETE MIXTURES

Mix ID	05850-0015v1	Custom Name	SMA				
Des.Level	SMA	Plant Code	PS00005850 - Madden Contracting - Port Allen, LA				
Mix Type	Wearing Course	Mix Temp	325	AC Corr Factor	-0.09	ADT	> 7000
Nom.Agg.Size	1/2 in.	Prod.Rate	350	Adj.Factor	1.00	Specs	2018/2021

	Supplier Code	Material Code	Custom Name	Agg %	Appr. Gravity	Bulk Grav.	Absp	FAA	Sand Eq	Flat Elng	CAA	Frictn Rate	Ret #4	Ret #8
C	APS00006880	1003M00120	P 78 SAND	24.0	2.662	2.560	1.5			1.0	100	I	74	91
C	APS00006880	1003M00120	PB 67M SA	19.0	2.664	2.575	1.3			0.9	100	I	80	93
C	APS00012880	1003M00120	#78'S	39.0	2.722	2.671	0.7			1.0	100	III	95	98
F	APS00006890	1003M00110	AGG LIME	18.0	2.704	2.647	0.8	48				III	0	1
Combined Aggregate Properties				100	2.693	2.622	1	48		1	100			

P/S	Material Code	Name	% Mix	Pass/Max Rut	LWT(des)	LWT(val)	SCB
APS00000400	1002M00050	PG76-22M	6.3	20000/6	3.04	4.4	0.85
PS00004680	1002M00230	FIBERS	0.30				
APS00011510	1002M00220	SP	0.07				

DESIGN		VALIDATION			
Parameter	Submittal	Average	Std.Dev.	PWL	JMF Limits
Gmm	2.421	2.424	0.002168	100	2.409 - 2.439
%Gmm,Ni	86.4	85.4	0.57009	100	Max 90.0
%Gmm,Nm					
Gmb,Nd	2.336	2.335	0.0038471		2.311 - 2.359
VMA	16.5	16.5	0.13038		Min 16.0
VFA	79	78	0.8367	100	69 - 80
%Voids	3.5	3.7	0.16432	100	2.5 - 4.5
% AC	6.3	6.2	0.07071		
Gse	2.663	2.662	0.0037149		
Pba	0.6	0.6	0.05362		
Pbe	5.7	5.6	0.04472		
Dust/Pbeff	1.47	1.42	0.068411		
Crushed	100	100	0	100	
Pass 1 1/2"	100	100	0	100	96 - 100
Pass 1"	100	100	0	100	96 - 100
Pass 3/4"	100	100	0	100	96 - 100
Pass 1/2"	91	92	1.5811		88 - 96
Pass 3/8"	72	73	0.8367		69 - 77
Pass No.4	31	33	0.5477		29 - 37
Pass No.8	23	23	0.8367	100	20 - 26
Pass No.16	20	20	0.8367		18 - 22
Pass No.30	16	17	0.7071		15 - 19
Pass No.50	13	14	0.5477		12 - 16
Pass No.100	11	12	0.5477		10 - 14
Pass No.200	8.4	8	0.39749	100	7.3 - 8.7

Submitted to District 61

Langley, Kent cmdc0018
Submitted By

4/12/2022
Date Submitted

Jennings, Cotina d61t7
Checked By

4/12/2022
Date Checked

Maher, Sean 00335891
Approved By

4/18/2022
Date Approved

00335891 Maher, Sean
Conditionally Validated By

7/18/2022
Date Validated

00335891 Maher, Sean
Validation Approval By

7/20/2022
Date Final Approved Validation

JMF of Mix 14

Lousiana Department of Transportation and Development
JMF SUPERPAVE ASPHALTIC CONCRETE MIXTURES

Mix ID	05850-0009v0	Custom Name	L1 BINDER				
Des.Level	1	Plant Code	PS00005850 - Madden Contracting - Port Allen, LA				
Mix Type	Binder Course	Mix Temp	325	AC Corr Factor	-0.11	ADT	3500 – 7000
Nom.Agg.Size	3/4 in.	Prod.Rate	350	Adj.Factor	1.00	Specs	2018

Supplier Code	Material Code	Custom Name	Agg %	Appr. Gravity	Bulk Grav.	Absp	FAA	Sand Eq	Flat Elng	CAA	Frictn Rate	Ret #4	Ret #8
	Combined Aggregate Properties		0										

P/S	Material Code	Name	% Mix	Pass/Max Rut	LWT(des)	LWT(val)	SCB
APS00000400	1002M00040	PG70-22M	4.2	20000/10	4.93		0.66
APS00000510	1002M00040	PG70-22M	---				
APS00011510	1002M00220	SP	0.10				

DESIGN		VALIDATION			
Parameter	Submittal	Average	Std.Dev.	PWL	JMF Limits
Gmm	2.508				2.493 - 2.523
%Gmm,Ni	88.3				Max 91.0
%Gmm,Nm	97.8				Max 98.0
Gmb,Nd	2.417				2.393 - 2.441
VMA	0				Min 12.5
VFA	0				69 - 80
%Voids	3.6				2.5 - 4.5
% AC	4.2				
Gse	2.676				
Pba	0				
Pbe	4.2				
Dust/Pbeff	0.93				
Crushed	99				
Pass 1 1/2"	100				96 - 100
Pass 1"	100				96 - 100
Pass 3/4"	98				94 - 100
Pass 1/2"	82				78 - 86
Pass 3/8"	65				61 - 69
Pass No.4	33				29 - 37
Pass No.8	27				24 - 30
Pass No.16	24				22 - 26
Pass No.30	22				20 - 24
Pass No.50	15				13 - 17
Pass No.100	7				5 - 9
Pass No.200	3.9				3.2 - 4.6

Submitted to District 61

Maher, Eric cmdc0026
Submitted By

2/4/2022
Date Submitted

Maher, Sean 00335891
Checked By

2/4/2022
Date Checked

Maher, Sean 00335891
Approved By

2/4/2022
Date Approved

Conditionally Validated By

Date Validated

Validation Approval By

Date Final Approved Validation